The Strontium Isotope Record of Zavkhan Terrane Carbonates: Strontium Isotope Stability Through the Ediacaran-Cambrian Transition

The Strontium Isotope Record of Zavkhan Terrane Carbonates: Strontium Isotope Stability through the Ediacaran-Cambrian Transition

A thesis presented

by

Tanya Petach

to

the School of Engineering and Applied Sciences

and the Department of Earth and Planetary Sciences

in partial fulfillment of the requirements

for a degree with honors

of Bachelor of Arts

April, 2015

Harvard College

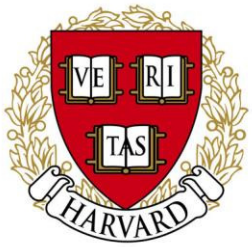

Abstract

First order trends in the strontium isotopic ($^{87}Sr/^{86}Sr$) composition of seawater are controlled by radiogenic inputs from the continent and non-radiogenic inputs from exchange at mid-ocean ridges. Carbonates precipitated in seawater preserve trace amounts of strontium that record this isotope ratio and therefore record the relative importance of mid-ocean ridge and weathering chemical inputs to sea water composition. It has been proposed that environmental changes during the Ediacaran-Cambrian transition may have enabled the rapid diversification of life commonly named the "Cambrian explosion." Proposed environmental changes include 2.5x increase in mid-ocean ridge spreading at the Ediacaran-Cambrian boundary and large continental fluxes sediment into oceans. These hypotheses rely on a poorly resolved strontium isotope curve to interpret Ediacran-Cambrian seawater chemistry. A refined strontium isotope curve through this time period may offer insight into the environmental conditions of the early Cambrian.

New age models and detailed mapping in the Zavkhan terrane in west-central Mongolia provide the context necessary for robust geochemical analysis. This study aims to better resolve the coarse strontium isotope curve for the early Cambrian period by analyzing carbonate sequences in the Zavkhan basin. These carbonate sections are rapidly deposited, have undergone little diagenesis, and are likely to preserve a primary seawater signal. Strontium isotope analysis of these sequences was carried out to determine changes in hydrothermal activity and weathering fluxes during this time period. Recompiling these data with a global dataset of strontium isotopes through this time period indicates a stable strontium isotope signal through much of the early Cambrian. These data do not support previous hypotheses attributing the driving mechanism for the early Cambrian transition from Mg-dominated to Ca-dominated seas to increased sea floor spreading rates.

Table of Contents

List of Figures

Acknowledgments

I would like to thank Francis Macdonald for both the opportunity to work on this project and the unwavering guidance throughout. His unending enthusiasm and insatiable curiosity have been a constant inspiration and reminder of why I love geology.

I owe an enormous thank you to Emmy Smith for her unparalleled patience while teaching (and re-teaching) me most of what I know about geology. She has been an incredible mentor through this project, as well as a steadfast supporter in my ability to complete it. Many thanks to her optimism, willingness to teach, and phenomenal company in the field.

A huge thank you to…

Sarah Dendy for teaching me the basics of strontium isotope analysis, helping run the Neptune mass spectrometer, and providing ceaseless support for the Macdonald Lab.

Alan Rooney for patient explanations of column chemistry, the occasional use of his hood space, and maintaining the Macdonald clean room.

Jurek Blusztajn and Woods Hole Oceanographic Institute for the use of their Neptune and help running it.

Blake Hodgin for surprising insights, inspiring conversations, and emergency help in the lab.

Dan Bradley and Sarah Moon for the months spent romping the Mongolian steppe together in search of sedimentary rocks. I truly owe you guys a lot of productive days and more than a little of my sanity.

Chenoweth Moffatt, Patrick Ulrich and the EPS & ESE department for unwavering support, funding, and tremendous quantities of tea and cookies.

INTRODUCTION

The geologic history of the Earth is divided into two major intervals: the Precambrian Supereon and the Phanerozoic Eon. The transition from the Ediacaran Period (the end of the Precambrian) to the Cambrian Period (the beginning of the Phanerozoic) at ~540 Ma is commonly portrayed as a time of flux, instability, and rapid change in Earth history. Perhaps most notable among these changes is the explosion of life manifested in the rapid diversification of body plans, the widespread development of exoskeletons, and the emergence of predation that all occur over a few tens of millions of years during the early Cambrian (Stanley, 1976; Knoll and Carroll, 1999). It has been proposed that environmental changes during the Ediacaran-Cambrian transition may have enabled the rapid diversification of life. The rise in atmospheric oxygen, for instance, is an imperative precursor to the development of large quantities of biologic activity. Low levels of oxygen early in Earth history may have presented a barrier to the development of large life forms (Knoll and Carroll, 1999; Sperling et al., 2013). Accompanying this notable and drastic change in the fossil record are a number of lithological and geochemical changes in the rock record including the increase in phosphorite deposits, glauconitic sandstone, molybdenum and uranium enriched shales, a transition from aragonitic to calcitic seas, and major fluctuations in the carbon cycle (Cook and Shergold 1986; Brasier et al., 1992; McKerrow et al., 1992; Kump, 1991; Mazumdar, 1999). These unusual indicators in the rock record are often attributed to tectonic drivers (e.g. Squire et al., 2006) or to changes in the Earth's dynamo and magnetic field (Kirschvink, 1997). Particularly, strontium isotope records have been used to support increased silicate weathering fluxes, increased hydrothermal activity, changes in the Mg/Ca, a transition from aragonite to calcite seas, and changes in eustatic sea level (Maloof et al., 2010; Dalziel et al., 2014; Peters and Gaines 2012; Derry et al., 1994).

Identifying paleo-environments can be tricky for a variety of reasons. During the Precambrian-Cambrian transition, the interpretation of paleo-environments is challenged by three limitations: (1) the lack of integrated high-resolution biological and environmental records (sedimentological and geochemical); (2) a robust and high-resolution age model for sediments through this time period; and, (3) uncertainties in precisely correlating between sections globally.

The strontium isotope system acts as a proxy for two of the aforementioned environmental changes that may be responsible for abnormal signals in the rock record: (1) the relative input of continental denudation and (2) hydrothermal activity. Changes in the Sr isotope composition and abundance of what is being weathered into the ocean, and changing the amount of Sr exchange at mid-ocean ridges should result in changes in the $^{87}Sr/^{86}Sr$ isotope ratio of precipitated carbonates, yet disentangling the combined effects of these two first order drivers is non-unique. This study initially aims to develop a strontium isotope curve through the early Cambrian that is (1) high resolution, (2) well-correlated with a robust age model, and (3) correlated with other contemporaneous sections globally. This strontium isotope data is then used to test whether the hypothesized environmental changes are consistent within the constraints of a high-resolution strontium isotope curve.

If the Ediacaran-Cambrian transition is associated with a dramatic increase in weathering flux (Peters and Gaines, 2012) the strontium isotope curve should record heavier (more radiogenic) values. If, on the other hand, the Ediacaran-Cambrian transition is associated with a 2.5x increase in mid-ocean ridge spreading (Maloof et al., 2010), the strontium isotope curve should record lighter (less radiogenic) values.

The Strontium Cycle

The strontium cycle on the Earth is recorded by the incorporation of strontium ions into carbonate lattice when calcium carbonate and magnesium carbonate precipitate from the water column. As strontium is an energetically unfavorable replacement for calcium (or magnesium) in carbonate lattice structures, strontium residence time in oceans is long (~10^6 years; Hodell, 1990). As this residence time is much longer than the timescale of complete ocean mixing, which occurs on the order of 10^3 years (MacArthur, 2012), strontium isotope values are typically inferred to record a global signature.

The strontium system is driven by an isotope fractionation of strontium between oceanic and continental crust. This fractionation occurs from the decay of ^{87}Rb to ^{87}Sr with a half-life of 48.8 Ga, older than the age of the universe (Davis et al., 1977). The continental crust inherently contains more ^{87}Rb than oceanic crust (a product of mantle differentiation) as it is typically much older than oceanic crusts (and therefore more ^{87}Rb has decayed into ^{87}Sr). Thus, continental crust accumulates higher ratios of $^{87}Sr/^{86}Sr$ than oceanic crust (continental crust has an average value around ~0.712, while hydrothermal inputs are typically ~0.7035). As strontium, both ^{87}Sr and ^{86}Sr, are released from hydrothermal vents and riverine weathering fluxes, a strontium reservoir builds up in the oceans with a specific strontium isotope signature that is indicative of the relative strength of these two fluxes. This ratio is preserved in precipitated carbonates.

The $^{87}Sr/^{86}Sr$ isotope record has changed over Earth history with changing interplay of mantle and weathering processes. Since approximately 500 Ma, the $^{87}Sr/^{86}Sr$ ratio of carbonates through time has the appearance of a large, lopsided trough with high values in the mid-Cambrian, low values through much of the Phanerozoic, and high values in the last 40 Ma (Edmond et al., 1992). Young strontium isotope values are measured primarily using foraminiferal carbonates,

belemnite guards, and brachiopod shells as these materials change visibly when altered and resist diagenesis well (Jones et al., 1994, Veizer et al., 1999, Farrell 1995). However, for dates prior to 500 Ma, the strontium isotope curve loses resolution. Prior to 500 Ma, the rock record contains few well-preserved shells, and strontium isotopes are instead determined from precipitated carbonates. Older whole-rock carbonates can be difficult to test for secondary alteration. Much of the strontium data compiled for the early to mid-Cambrian is fraught with scatter. Additionally, many of the assumptions upholding the strontium isotope system fall into question in deep time. For example, was the residence time of strontium always ~2 Ma? Possible confounding factors include changing redox states of oceans, ion concentrations in seawater, and salinity. Previous work indicates that strontium isotope ratios are homogeneous in oceans with salinities as low as 20 psu (DePaolo and Ingram, 1985), and therefore, salinity should not have a large effect on the strontium isotope system of the early Cambrian relative to other confounding factors.

The strontium isotope signature is additionally complicated by the $^{87}Sr/^{86}Sr$ of the material weathered into riverine fluxes. Weathering young, volcanic materials or large volumes of carbonate rocks can create a memory effect of strontium isotope records (Brass, 1976). Other complications in interpreting the strontium isotope curve include post-depositional leaching, pore-water exchange, low-temperature metamorphism, or dolomitization. As a result, it is challenging to extract reliable strontium isotopes from old carbonates. Despite these challenges, a composite strontium isotope record for the early Cambrian (541-517 Ma) has been coarsely developed using data from Morocco (Maloof et al., 2010), Mongolia (Brasier et al., 1996), Siberia (Derry et al., 1994; Knoll et al., 1995, Nicholas 1996; Kaufman et al., 1996), and South China (Ishikawa et al., 2008; Sawaki et al., 2008).

Well-preserved sections in southwestern Mongolia show few signs of diagenesis and metamorphism. In this study, data from these sections with minimal

alterations are used to produce a strontium isotope curve through the early Cambrian and integrate it with other sections globally using a new age model. The strontium curve created from these carbonates can be used to test environmental changes in the early Cambrian. In particular, we use a newly developed and compiled composite strontium curve to test the hypothesis that a 2.5 fold increase in mid-ocean ridge spreading occurred during the early Cambrian (Maloof et al., 2010) and that the early Cambrian is characterized by a change in sediment inputs (Peters and Gaines, 2012; Derry et al., 1994).

GEOLOGIC CONTEXT

Geologic Timescales and Nomenclature

It is important to note that this research uses the Siberian nomenclature for the stages of the Cambrian Period (Nemakit-Daldynian, Tommotian, Atdabanian, Botomian, and Toyonian). Stages are used as the globally defined divisions of the early Cambrian. The globally defined stages 2-4 remain undefined in the Cambrian and much of the previous global Cambrian geochemical data compilations have been correlated using Siberian nomenclature (Maloof et al., 2010; Smith et al., in review). Prior work on these Mongolia sections utilize Siberian nomenclature (Brasier et al., 1996a; Brasier et al., 1996b; Goldring and Jensen, 1996; Khomentovsky and Gibsher, 1996), and thus for the sake of consistency with previous work, I also use Siberian nomenclature throughout this research (Figure 1).

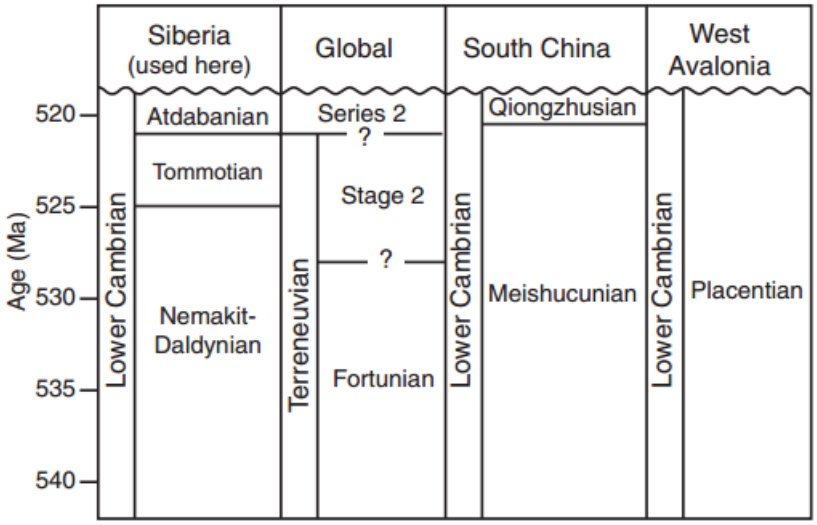

Figure 1. Lower Cambrian Stratigraphic Nomenclature. Figure from Maloof et al. (2010). Global standard names from the International Stratigraphic Chart (2009), boundary ages for Siberia are from Maloof et al. (2005; 2010a), and correlations with South China and West Avalonia are tentative and from Steiner et al. (2007).

Zavkhan Terrane

Prior to Mongolia's re-opened borders in 1994, the majroity of the geologic research in the Zavkhan terrane was conducted by Mongolian and Russian scientists. The Zavkhan terrane was first described by Bezzubtsev in 1963, and detailed follow-up work was not undertaken until the 1990s. Preliminary maps and stratigraphic descriptions were created by Voronin et al. (1982), Gibsher and Khomentovsky (1990), Gibsher et al. (1991), and Khomentovsky and Gibsher (1996).

In 1993, a research team, as part of the IGCP Project 303, "Precambrian-Cambrian Event Stratigraphy," visited localities in the Zavkhan basin and published the first geochemical curves through the Zavkhan terrane stratigraphy. In their research, they defined new unit boundaries, presented reconnaissance mapping,

measured preliminary low-resolution (10-20m) stable isotope chemostratigraphy, and correlated biostratigraphy (Brasier et al., 1996a; Brasier et al., 1996b; Goldring and Jensen, 1996; Khomentovsky and Gibsher, 1996; Kruse et al., 1996; Lindsay et al., 1996a; Lindsay et al., 1996b).

Geologic Background

Syntheses of the tectonic evolution of Mongolia have divided the country into 44 terranes accreted between S. China, Tarim, and Siberia during the Paleozoic (Badarch, 2002). One such structurally delineated terrane is the Zavkhan terrane located in the Altai Province, west of the town of Altai in the Zavkhan mountain range in the central Mongolian province of Gobi-Altai (Figure 2). The Zavkhan terrane is composed predominantly of Neoproterozoic and early Phanerozoic rocks (Macdonald et al., 2009; Lindsay et al., 1996).

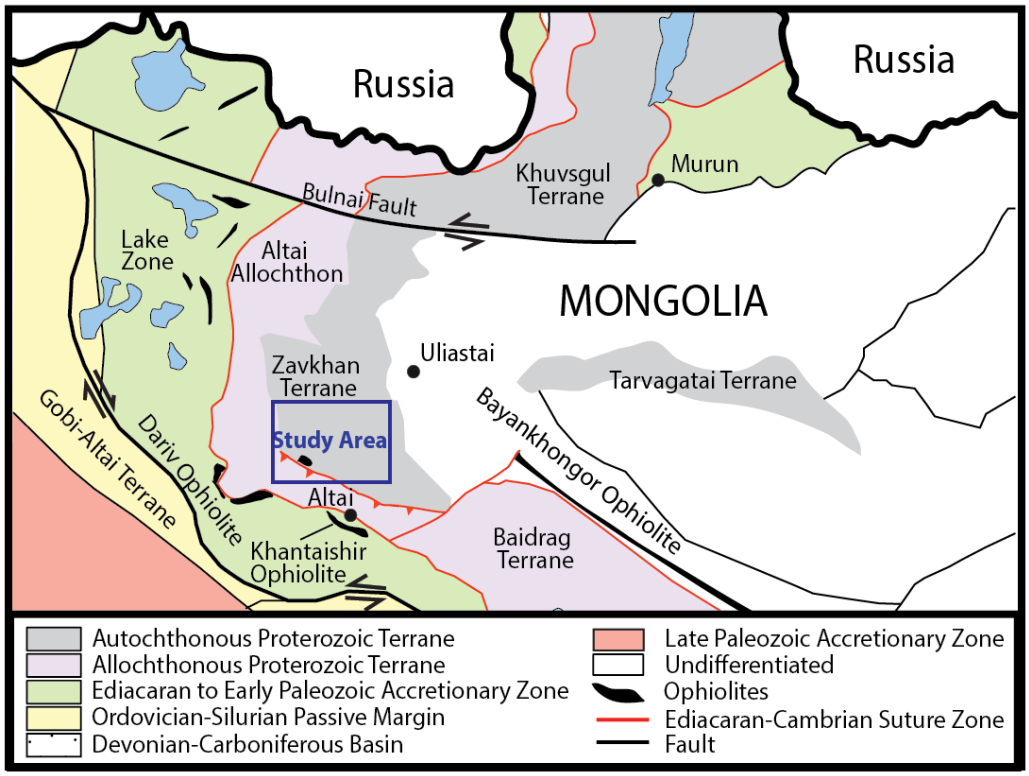

Figure 2. Map of Zavkhan terrane. Smith et al. (in review). The Zavkhan terrane is locates in the southwest Gobi-Altai province of Mongolia. The study area is highlighted in blue and a detailed geologic map of that area is shown in Fig. 7.

Previous work has divided the structure of the Zavkhan terrane into three distinct fault regimes that cut through the stratigraphy of the Zavkhan terrane: (1) thrust faults that formed during the compressional regimes of the Ediacaran-Ordovician record the accretion of terranes to the south (Gibson et al., 2013); (2) extensional faults that formed during the late Ordovician-Silurian in response to slab reversal (Kroner et al., 2010); and (3) dextral strike-slip faults that record the collision of S. China with the Mongolian terranes during the Devonian-early Permian (Lehmann et al., 2010). It has been suggested that the Zavkhan terrane is underlain by Archean and Proterozoic crystalline amphibolites, marbles, gneisses, and quartzites (Badarch, 2002; Dorjnamjaa and Bat-Ireedui, 1991), but these

metamorphic rocks are not exposed on the autochthon, and this inference rests solely on correlations with exposures on other terranes.

The upper stratigraphy of the Zavkhan terrane is dominated by thick, mixed carbonate and siliciclastic sedimentary sequences. Subsidence rates are interpreted to drastically increase on the Zavkhan terrane during the late Ediacaran-early Cambrian and accommodate rapid sedimentation. These Ediacaran and Cambrian sedimentary sequences of the Zavkhan terrane are interpreted to be deposited in a foreland basin (Macdonald et al., 2009) during the latest Ediacaran to early Cambrian as the result of the subduction of the Zavkhan terrane underneath the Khantaishir-Dariv Arc to the southwest (Macdonald et al., 2009; Smith et al., in review).

Stratigraphy of Upper Zavkhan Terrane

The stratigraphic nomenclature the Zavkhan terrane was recently refined (Bold et al., 2013). Ediacaran to Cambrian sediments in the Zavkhan terrane are composed of the Shuurgat, Zuun-Arts, Bayangol, Salaagol, and Khairkhan formations. The basal contact of the Zuun-Arts Formation (recently changed from the Zuun-Arts Member) is defined as a karst surface at the top of the Shuurgat Formation (Bold et al., 2013). The overlying sediments of the basal Zuun-Arts Formation are composed of massively bedded pink to buff colored dolostone with columnar stromatolites (Boxonia grumulosa) and chert nodules (Markova et al., 1972; Macdonald et al., 2009). The stromatolitic dolostone is overlain by phosphatic shale with interspersed carbonate nodules thought to represent a sharp transgressive sequence followed by a thinly bedded limestone. The upper horizons in the Zuun-Arts Formation mark the top of a large shallowing up sequence that terminates in crossbedded limestone with notable white and black ooids (Smith et al., in review).

The Bayangol Formation is divided into 5 members, Bayangol 2-6 (Smith et al., in review). The bottom contact is the sharp horizon between the crossbedded white and black ooid limestone of the Zuun-Arts Formation and the basal phosphatic shale of the Bayangol Formation. The Bayangol Formation undergoes dramatic lithologic and facies variation across the Zavkhan terrane. Each subunit (2-6) is capped by a sharp transition from mixed siliciclastic and carbonate units to a massively bedded limestone. Fossils (both ichnofauna and small shelly fossils) are abundant throughout the formation.

The Salaagol Formation is composed of a massively bedded archaeocyath reef ranging from gray to red in color. Other bioclastic debris is interspersed within the archaeocyath reef. The formation is inconsistently interbedded with silts and conglomerates.

The youngest formation on the Zavkhan terrane is the Khairkhan Formation. Composed of a diverse range of mixed siltstone, sandstone, and conglomerate, the Khairkhan Formation also contains city-block scale olistoliths of Salaagol Formation and carbonate and chert from unknown provenance. Additionally, the Khairkhan Formation contains clasts of ultramafics, bolstering the claim that these units were deposited in a foreland basin (Smith et al., in review). This formation is interpreted as the flysch and molasse in the closing of the foreland basin (Macdonald, 2009).

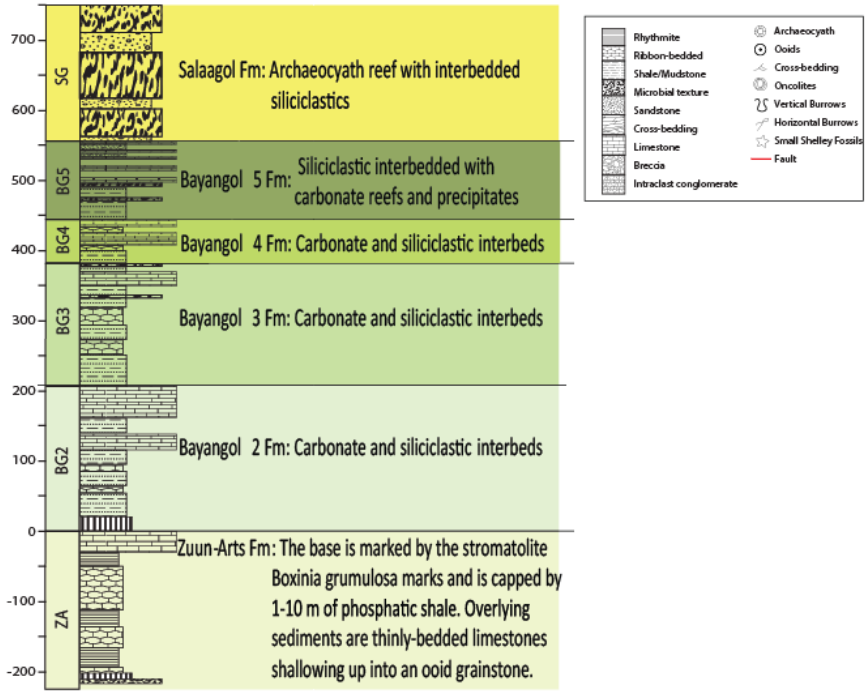

Figure 3. Stratigraphy of the late Ediacaran-Cambrian sediments in the Zavkhan terrane.

Age Model

Dating the Mongolian stratigraphy directly is challenging as no volcanic ashes have been discovered in these strata. As a result, the stratigraphy must be correlated with carbonate-dominated stratigraphy of a similar age elsewhere with interbedded ash horizons. These ash horizons can be dated and the Mongolian stratigraphy can be correlated with these precise dates using carbon isotope chemostratigraphy. The age model used to correlate the strontium isotopes in this study was constructed in Smith et al. (in review) using carbon isotopes correlation with Moroccan, Siberian and Chinese sections that are well constrained by U/Pb dates (Maloof et al., 2005; Maloof et al., 2010; Kouchinsky et al., 2007; Brasier et

al., 1996; Corsetti & Hagadorn, 2000; Narbonne et al., 1994). The carbon isotope curve from the Mongolian sections was created in parallel with this strontium isotope analysis, thus no correlation was required between the strontium data discussed here and the Zavkhan terrane age model. Two notable revisions from previous age models in the Zavkhan terrane include: (1) the Bayangol Formation is entirely composed of Nemakit-Daldynian sediments (ca. 540-538 Ma), and (2) the Salaagol Formation is Tommotian in age (ca. 524-522 Ma).

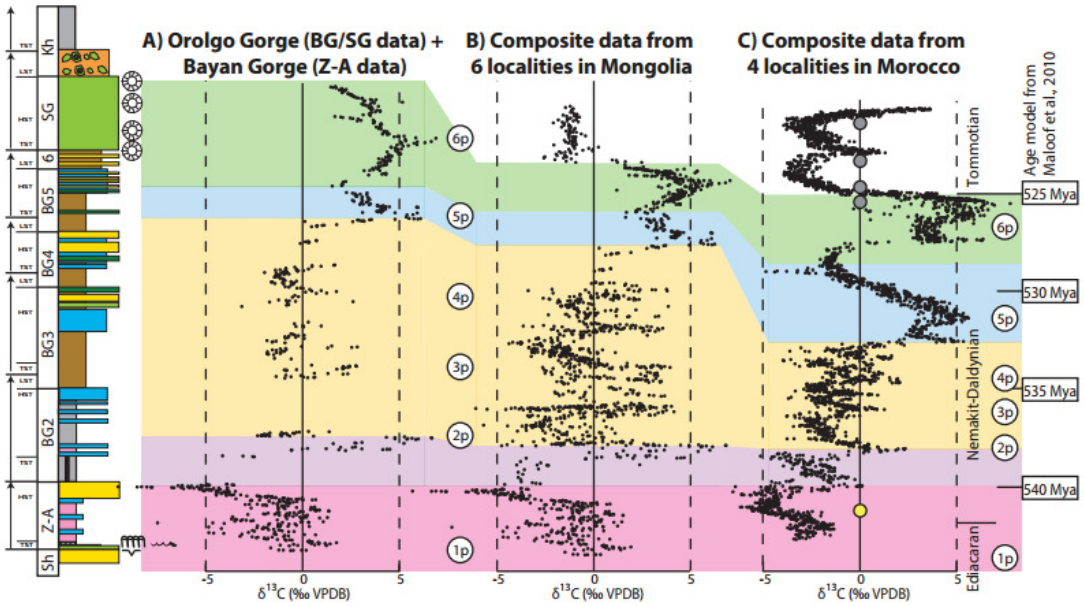

Figure 4. Smith et al., in review Age Model. Carbon isotope peaks were matched between global sections to correlate the Mongolian stratigraphy to Moroccan and Chinese sections with good age constraints. Note that the Morocco dates are U/Pb zircon ages (Maloof et al., 2005).

PREVIOUS EARLY CAMBRIAN Sr ISOTOPE COMPILATIONS

The first order strontium isotope curve follows a basic trend of changing mid-ocean ridge spreading and weathering rates. Data from the past ~500 Ma resemble a large trough. Strontium values have increased for the past ~150 Ma in large part due to the Himalayan orogeny (Edmond, 1992). Strontium isotopes through the early Cambrian are perturbed by a previously described negative excursion (Figure 5).

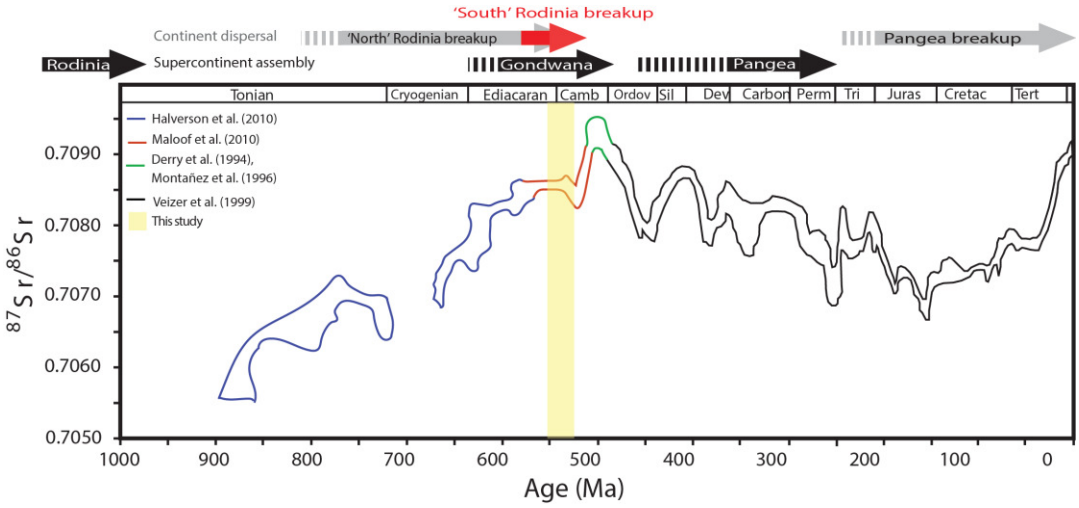

Figure 5. Strontium isotopes through time. Adapted from Maloof et al., 2010. Note that the time period examined in this study is highlighted in yellow. Data are sparse through the Cryogenian due to Snowball Earth periods.

Previous strontium isotopes compilations in the early Cambrian are prone to error from both age model construction and large scatter in data. These compilations therefore have a diverse range of interpretations, perhaps due to the low resolution and high variability in the data collection. Prior strontium isotopes were measured in the Zavkhan terrane by Brasier et al. in 1996. The Brasier strontium curve indicates that the $^{87}Sr/^{86}Sr$ ratio increases drastically during the late Neoproterozoic but remains relatively stable through the early Cambrian (Figure

6). The localities of these data are well documented. Our detailed mapping indicates that there are numerous discrepancies in the mapping and stratigraphic sections measured in the Brasier et al., 1996 work. Smith et al. (in review) re-mapped many of Brasier's localities and made both lithologic and stratigraphic height alterations in previously measured sections. These changes were due to a combination of mis-mapped carbonates and measured sections over minor faults that repeat or eliminate stratigraphy.

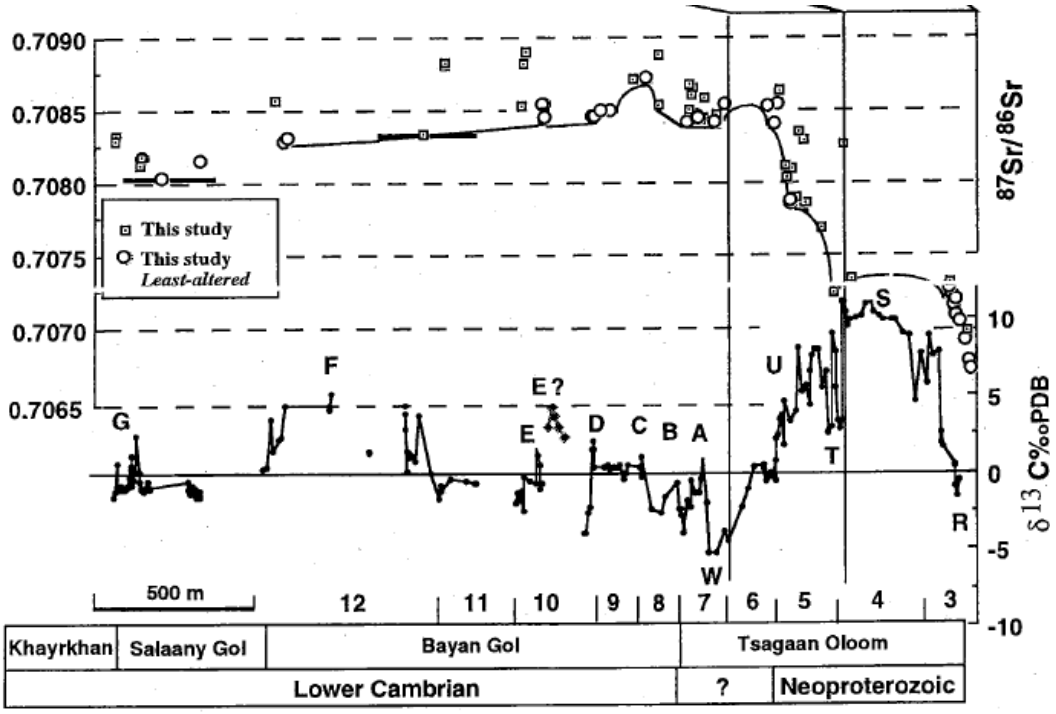

Figure 6. Strontium and carbon isotopes from the Zavkhan terrane. Brasier et al., 1996. Detailed mapping carried out with this study indicates that many of Brasier's measured sections were in misplotted rock units. Samples from the KTN locality, for instance, were mapped as Bayangol, but are located in the Saalagol formation.

The early Cambrian strontium isotope curve has been measured in sections worldwide (Derry et al., 1994; Brasier et al., 1996; Maloof et al., 2010). Strontium isotopes measured from early Cambrian sections in Siberia demonstrate a sharp

increase in strontium isotope ratios in the ten million years following the start of the Cambrian period (Derry et al., 1994). These data have been interpreted as a response to the breakup and weathering of the Pan-African Orogeny (Derry et al., 1994).

Similar work in Svalbard, Namibia, NW Canada, and Greenland also indicate a long-term increase in strontium isotope values throughout the early Cambrian period (Figure 5; Kaufman et al., 1993). The Svalbard, NW Canada, and Greenland data, unlike the Siberia data, suggest that the majority of the increase in strontium isotope ratios occurs during the Ediacaran (635-540 Ma) as a result of the Pan-African Orogeny, and indicate that strontium isotope values were relatively stable during the Cambrian Period (Figure 7; Kaufman et al., 1993; Derry et al., 1994).

A recent composite section composed by Maloof et al. (2010) further complicates the understanding of environmental changes during the early Cambrian. The composite curve is interpreted to represent a decrease in global strontium isotope values throughout the early Cambrian (Figure 7; Maloof et al., 2010). This decreasing trend was interpreted to be the result of seafloor spreading.

Here we refine the strontium isotope record from late Ediacaran and early Cambrian strata in Mongolia to reconcile these two interpretations: Does the Ediacaran-Cambrian transition record a rise or fall in strontium isotopes and how does this relate to proposed environmental change?

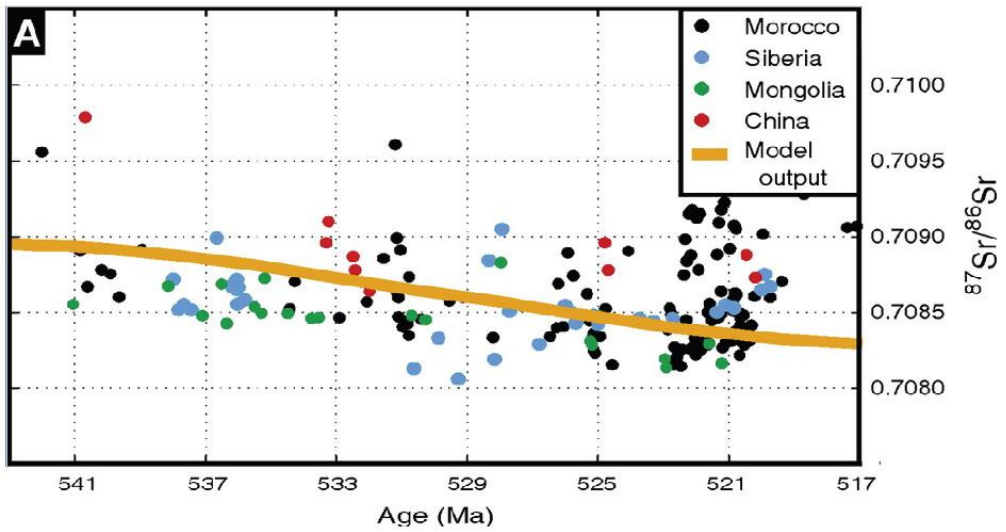

Figure 7. Composite curve of strontium isotopes through the early Cambrian. (Maloof et al., 2010). These data were interpreted to represent a smooth, decreasing strontium isotope signal that follows the predicted model output.

METHODS

Geologic Mapping, Measuring Stratigraphic Sections, and Sampling

The geologic mapping for this study was carried out in relevant areas within the Zavkhan terrane over summer 2011-2013 field seasons. This study is dependent upon knowing both the strontium isotope ratio and the stratigraphic position of each sample. To ensure that the depositional environment of each sample was known, extensive mapping and careful measuring of stratigraphic sections was carried out.

Sections were measured in the field, and samples were collected at approximate 1m intervals. Least altered samples were collected in the field, and care was taken to ensure that samples had high carbonate content and minimal diagenesis (e.g. samples with calcite or quartz veins were avoided). Detailed notes were taken on the ~1m scale to record the identity of overlying and underlying strata, sedimentary textures, and contacts above and below each sampled bed. Samples from six sections were collected for strontium isotopes (Figure 8). These sections are E1129, E1207, E1220, E1138, E1211, and E1216.

Strontium Isotope Analysis

Samples were cut to expose fresh surfaces and drilled with a tungsten carbide drill bit to powder least altered horizons for strontium analysis. Approximately 50 mg of powder was drilled from each sample. Care was taken to avoid any altered textures in samples, and the finest grained material was targeted. To remove excess clay particulate, powdered material was eluted in methanol (1:1), shaken vigorously, and sonicated for 12 minutes. After sonication, the solution was decanted, and the procedure was repeated a total of three times. This process was conducted first with methanol, then ammonium acetate (0.5M), and finally

deionized water. Samples were finally dissolved in acetic acid and transferred to heat-resistant Teflon vials.

Samples underwent a two-step reflux process to remove acetic acid and were then dissolved in pure nitric acid. After evaporating the acetic acid, samples were left for 8 hours in a solution of 3N nitric acid. The nitric acid was then evaporated, and the process was repeated. Finally, samples were passed through strontium columns to remove similarly sized ions (e.g. Rb) from the samples. Columns were also eluted using varying concentrations of nitric acid. A final rinse of the columns with deionized water freed strontium ions into a collection vial. These samples were dried and re-eluted.

The final strontium samples were analyzed by inductively coupled plasma mass spectrometry using a Neptune inductively coupled plasma mass spectrometer (ICP-MS) to determine strontium ion concentrations. In all cases blanks and duplicates were run with the strontium samples. Samples were corrected with external standards that have well documented $^{87}Sr/^{86}Sr$ ratios. A mean $^{87}Sr/^{86}Sr$ ratio is determined after standards are measured multiple times on the spectrometer. Data are corrected to the difference between expected and actual values on these standards. Outlier points were re-analyzed. On outlier points, hand samples with data were determined to be reproducible within $1.22e^{-5}$.

Major Element Analysis

Samples were powdered and sent to the Vancouver branch of SGS labs for major element composition. Samples sent out for major element analysis are whole-rock samples of the same aliquot of powder but not the same dissolution from which the strontium isotopes were measured. At the SGS labs, samples were dissolved using a two-acid digestion of HCl and HNO_3 and run on an ICP-MS for major element constituents.

RESULTS

Geological Mapping and Interpretations

The detailed map created during the field seasons documents new structures in regions surrounding measured sections. Sections were measured across the basin, and strontium analysis was performed on samples from six sections. Samples measured for strontium isotope ratios are E1220, E1129, E1207, E1138, E1211, and E1216. The relative locations of these sections are illustrated in the map in Figure 8. Note that mapping for other sections analyzed is published in Smith et al. (in review). On all maps, the Bayangol Formation is mapped as six distinct members (Bayangol 2-6).

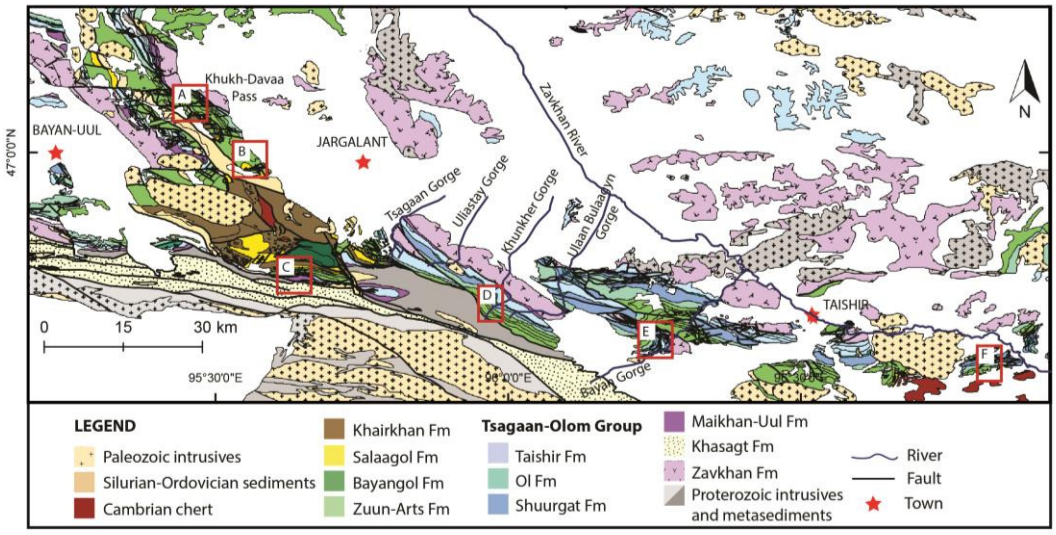

Figure 8. Map of sections for analyzed samples. Smith et al., in review. A. NE Khukh Davaa (section E1211); B. SE Khukh Davaa (section E1209); C. Orolgo Gorge (section E1220); D. Khunkher Gorge (section E1138); E. Bayan Gorge (section E1129); F. KTN (section E1216).

Section E1220, the thickest and most distal section extending from the basal Bayangol Formation contact through the upper Salaagol Formation, was mapped in

extensive detail for this project. As a result of the high deposition rate, the good exposure, and the detailed section measurements, the majority of the strontium isotope samples analyzed are from section E1220. A detailed map of section E1220 is shown in Figure 9.

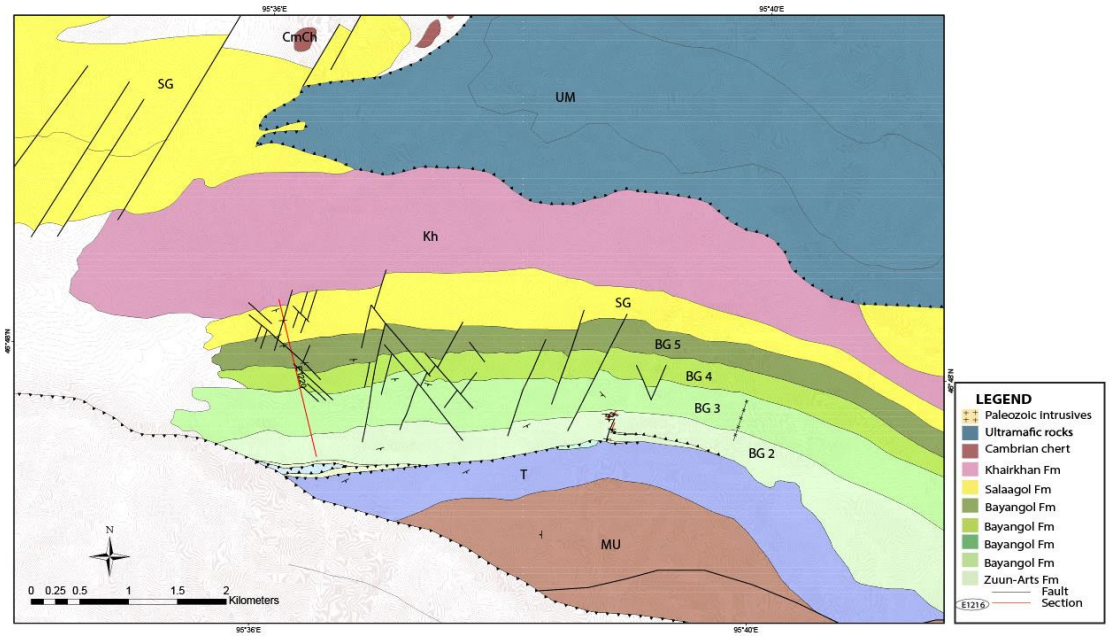

Figure 9. Map of Orolgo Gorge (E1220) Section. Mapped by Smith and Petach. Note the two dominant fault structures cutting through the section. Olistoliths in the Khairkhan Formation are often >0.5km in length.

Strontium Isotopes

Forty-five samples from the Zuun-Arts and Bayangol formations were analyzed for strontium isotopes. These samples were taken from sections spanning the Zuun-Arts through Salaagol formations. Samples of the Zuun-Arts Formation were taken from Section E1216 (KTN locality) and E1129 (S.E. of Bayan gorge). Bayangol Formation samples used in this study are from E1138 (Khunkher Gorge), E1211 (NE Khukh Davaa), E1220 (Orolgo Gorge) and E1207 (SE Khukh Davaa).

Salaagol Formation samples were taken from E1220 (Orolgo Gorge). The strontium values of these sections are plotted alongside carbon isotope curves in Figure 10.

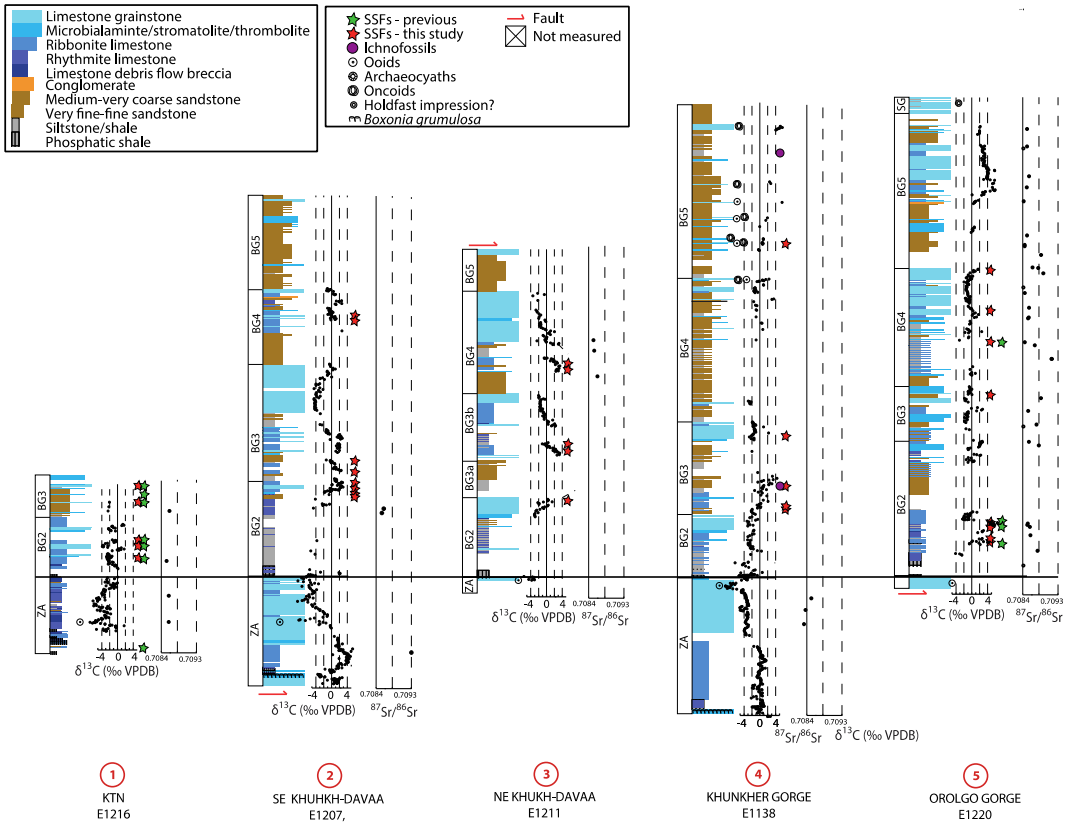

Figure 10. Strontium and carbon isotopes plotted against stratigraphic height. Note that all stratigraphic sections and carbon isotope curves are from Smith et al. (in review).

$^{87}Sr/^{86}Sr$ values were measured between 540-525 Ma. The values are predominantly between 0.7084-0.7087. Compared with the modern Sr value of ~0.7091 and the global nadir in the Permian of ~0.7068 (Burke et al., 1982), this variation between 0.7084-0.7087 represents approximately 10% of the total global

variation over the past 500 Ma. The variations occur on short timescales and the overall trend is stable through the late Ediacaran to early Cambrian.

The three samples taken from the E1129 Zuun-Arts section have strontium isotope values that range from 0.70845 to 0.70849. These values are comparable with Zuun-Arts samples taken from E1216 at the KTN locality that range from 0.70849 to 0.70857.

Samples taken from the Bayangol Formation section E1138 have strontium values that start at 0.70850 and become lighter up section until reaching a value of 0.70871. The three samples from Bayangol Formation E1207 range from 0.70855 to 0.70930, but do not exhibit any overall trend. Bayangol E1211 samples similarly range from 0.70849 to 0.70860.

The majority of samples analyzed in this study are from the Bayangol and Saalagol formations in section E1220. These strontium isotope values near the base of the Bayangol formation have values ~0.70877. The isotope curve exhibits some variation up section through the E1220 stratigraphy. However, the majority of the isotope values lie between 0.7084-0.7087. The upper stratigraphy in this section is dominated by strontium isotope values around 0.7085.

Vetting Samples

Traditionally, strontium isotope samples are vetted according to their texture, strontium content, rubidium content, silicate mineral content (aluminum, iron, and magnesium), and $\delta^{18}O$ (Kaufman et al., 1993; Nicholas et al., 1993; Moore 1989; Halverson et al., 2007). These criteria indicate the presence of clay minerals (which often release radiogenic strontium into the surrounding carbonate matrix), diagenetic fluid flow (which enables strontium ion exchange between meteoric water and host rock), and metamorphic alteration (which may preferentially preserve or discard certain elements). The applicability of these vetting criteria to

the early Cambrian is suspect; however, data were screened using these criteria as an experiment to determine which samples would be screened. Vetting criteria in this study were set at standard levels across the entire data set (Figure 11). Samples [Mg] > 1%, [Mn] > 750ppm, [Sr] < 500ppm, Fe/Sr > 3, and [carbonate] < 85% were screened from the dataset. These levels are determined to be conservative cutoff values for typical strontium analysis. The data are re-plotted in Figure 12.

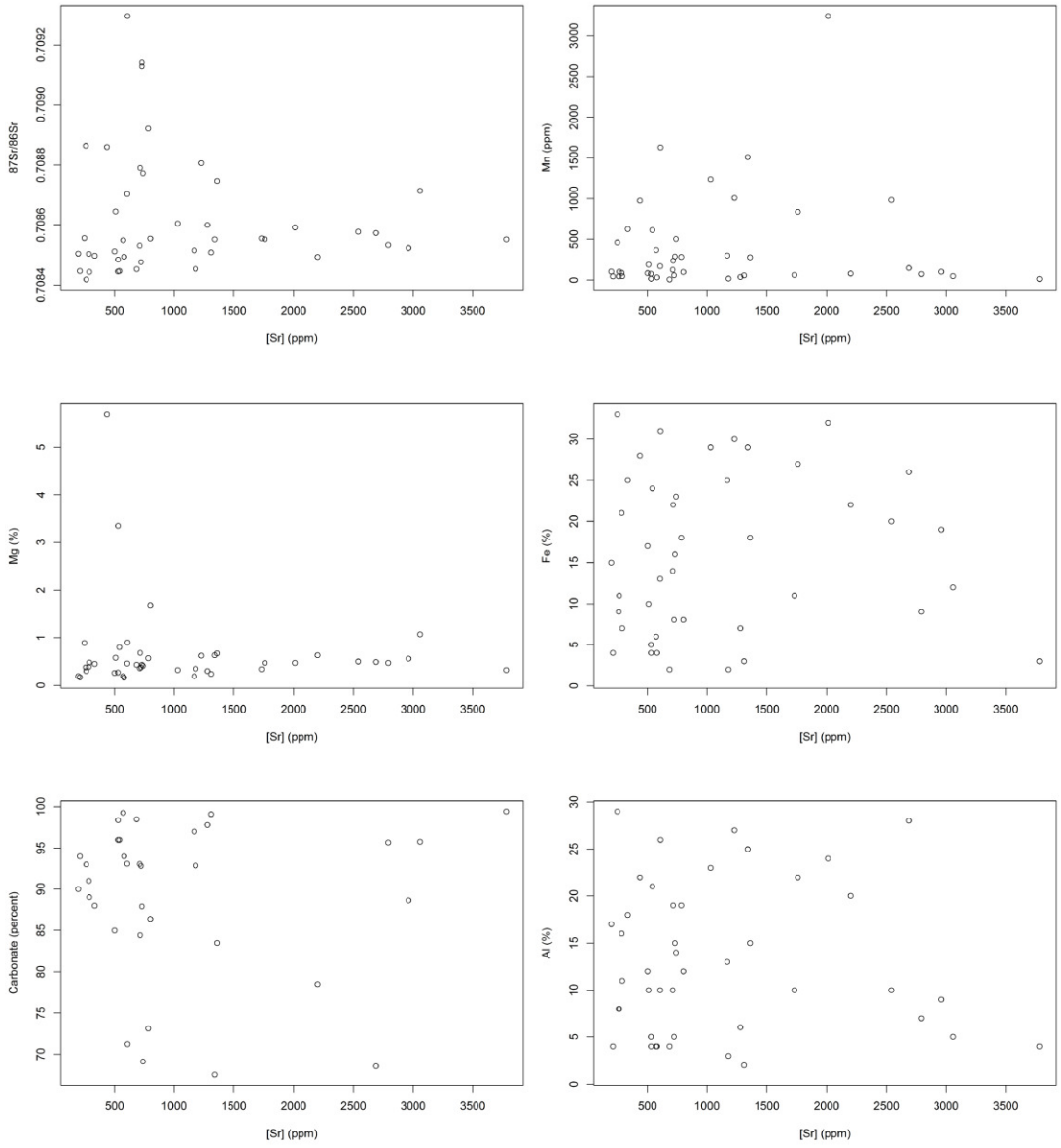

Figure 11. Standard vetting criteria for strontium isotopes. Note the enormous scatter on the Sr-vs-Fe and Sr-vs-Al graphs. The trend on the Sr-vs-$^{87}Sr/^{86}Sr$ is also poorly correlated.

To determine if screening criteria were useful, data cutoffs for least altered samples were set specifically for each elemental analysis. In least altered samples, concentration of magnesium is less than 1%, manganese less than 750ppm, an iron to strontium ratio less than 5, aluminum less than 1%, and Sr concentrations greater than 500 ppm. Additionally, samples with carbonate content less that 85% were screened out of the data set.

The samples removed by these vetting criteria were not always samples with high strontium isotope ratios. Samples measured at 534.35 Ma (arbitrary stratigraphic height 410m in Figure 12), for instance, are not removed from the data set by these traditional vetting criteria. Despite the decrease in data density after the screening process, the scatter of the data is not greatly diminished.

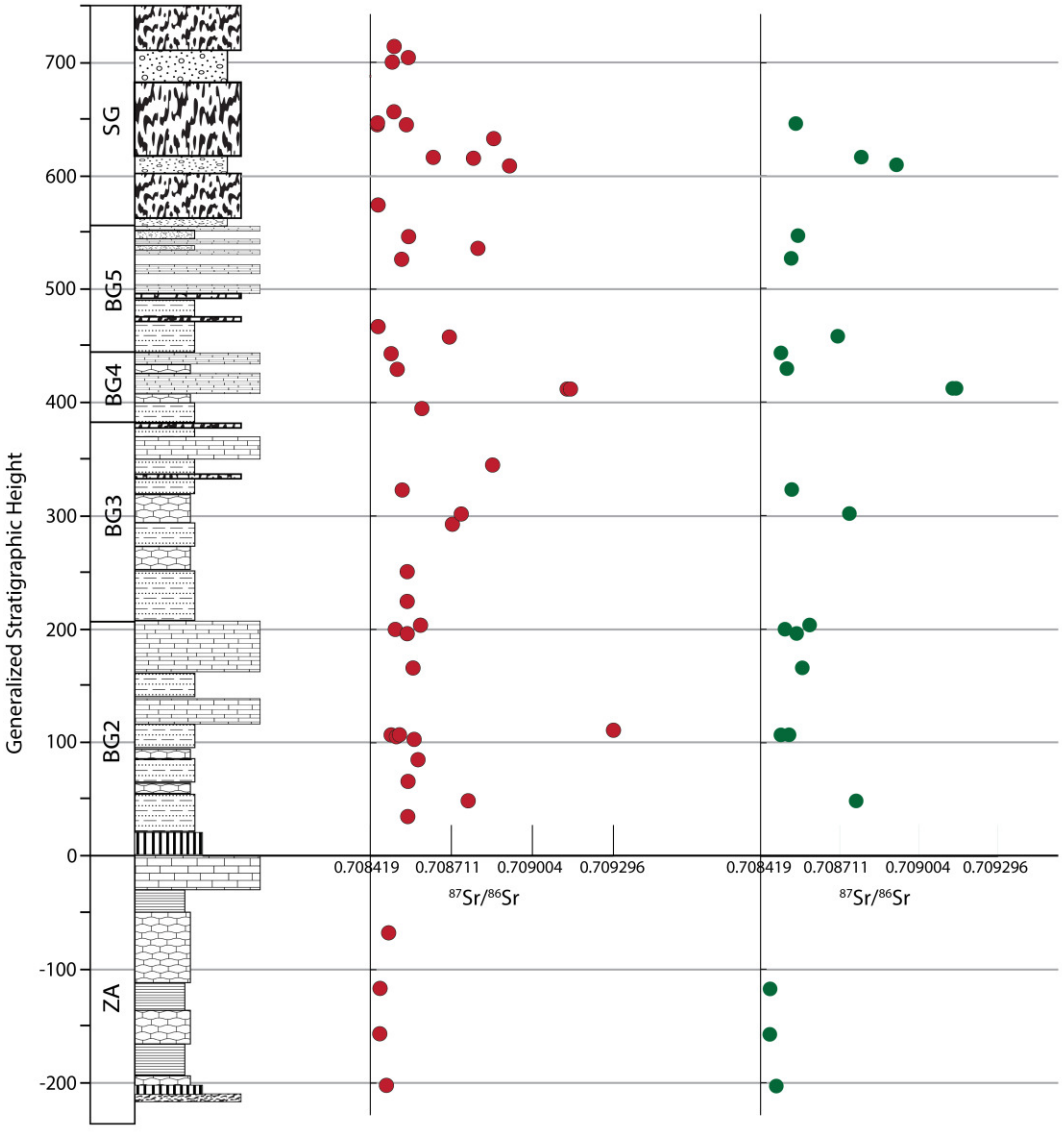

Figure 12. Screened and raw data plotted against generalized stratigraphic height. Note that many of the most extreme outliers are not screened with the traditional vetting criteria, but many of the middle points were removed. The screening tests have homogeneously diminished the data set size without eliminating scatter.

Samples were then examined for evidence of diagenesis. Samples with no evidence for diagenesis and carbonate content > 85% are reported in the composite Mongolia Sr curve (see discussion for more detail).

Composite Sr Curve from Mongolia Stratigraphy

These sections were tied to one another using unit contacts and marker beds to create composite sections. Strontium isotope values begin ~0.7087 at the base of the sections and remain stable around ~0.70875 between 541-536 Ma. Samples between 536-534Ma record increased variability with values ranging between 0.7091-0.7084 on short time intervals. Isotope values follow a gradual increase between 534-530 Ma to a peak of 0.7092 at 530.6 Ma. Isotope concentrations fall rapidly following the 530.6 peak to ~0.7085 where they remain stable for the upper stratigraphy in the section.

It is difficult to identify altered strontium isotope samples. There are three striking outlier data points on the $^{87}Sr/^{86}Sr$ plot for these sections at 535.1 Ma, 534.3 Ma, and 529.6 Ma (Figure 13). To determine the reliability of these data points, samples were vetted using traditional criteria (presence of clay-indicating elements), examinations for diagenetic alterations, and carbonate content. Importantly, many of the radiogenic fliers show no evidence of diagenesis.

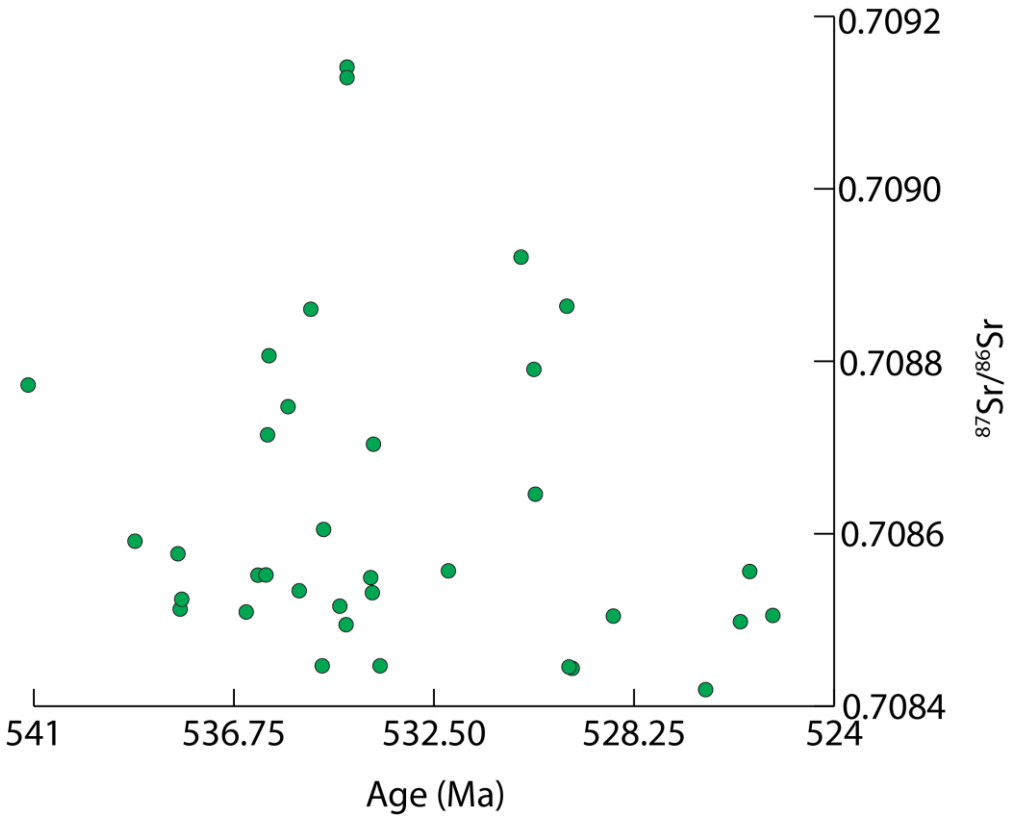

Figure 13. Plot of strontium isotope data with age. Lowest value trends indicate a fairly flat trend through the 17 Ma plotted.

DISCUSSION

Strontium Isotopes through the Cambrian

The strontium isotope curve is interpreted as the trend set by the lowest recorded values. As $^{87}Sr/^{86}Sr$ ratios are altered through meteoric water ion exchange and rubidium decay, the concentration of ^{87}Sr increases in carbonates through time. Few processes artificially increase the concentration of ^{86}Sr over time. Thus older carbonates are prone to have artificially increased strontium isotope ratios. As a result, the lowest values on the strontium isotope record are interpreted to record the "most reliable" values. The strontium isotope curve through time can be traced in a plot by following the trend of the lowest $^{87}Sr/^{86}Sr$ values through time.

The strontium isotope curve throughout the early Cambrian, as recorded in the six interpreted Zavkhan sections, is relatively stable between 540-525 Ma. Perhaps more striking, these data do not appear to follow a long-term increasing or decreasing trend. While the data are relatively stable through the time period examined, there are some excursions in the data. Some of these perturbations are poorly resolved and it is difficult to determine if these high ^{87}Sr data points are the result of diagenesis. These data are prone to high scatter. As most strontium alteration increases the $^{87}Sr/^{86}Sr$ ratio of the strontium incorporated into the lattice, the first order "flat" trend of the strontium isotopes through this time period is inferred from the lowest values.

During the incorporation of the Zavkhan terrane strontium isotope values with a global compilation, care was taken to ensure the age models are appropriately linked. To appropriately plot both the Brasier (1996) Mongolia dataset and data from this study, we propose two changes to the Maloof (2010) global strontium isotope curve for the early Cambrian: (1) the addition of our strontium isotope data to the curve, and (2) minor changes to the age models used

in two of the Maloof (2010) sections. These sections are: Brasier (1996) sections from the Kvete-Tsakhir-Nuruu locality and four data points from the Siberia-Kotuikan section which have appropriate age model dates in the SOM data for the Maloof (2010) dataset, but appear to be mis-plotted on the curve. The Brasier, (1996) KTN section is predominantly Salaagol Formation limestone, which we date between 528-525 Ma in our age model; these data were moved from Maloof's age of 533 Ma to these younger, refined age model dates in the modified composite section. The Siberia data are plotted with dates Maloof cites in his SOM data.

The upper Zavkhan terrane strontium isotopes section offer new insights and increased resolution for the strontium record through the earliest Cambrian. Previous Nemakit-Daldynian through Atdabanian age strontium isotopes have high variability and are not singularly interpretable (Derry et al., 1994; Maloof et al., 2010; Shields et al., 2002). Strontium isotopes from the upper Zavkhan terrane stratigraphy indicate stable relative hydrothermal activity and weathering inputs during early Cambrian environments. The stability of these data is curious, as the early Cambrian has been interpreted to record the weathering signal of the Pan-African orogeny or increased weathering from the Sauk transgression above the great unconformity. The orogenic signal may still be present in the sediments, but may resolve itself on a different timescale than the 25 Ma examined in this study. The Himalayan orogeny, for instance, is well recorded in strontium isotopes on timescales both <<25 Ma and in a long upward trend in strontium isotopes that still continues today (Edmond, 1992).

Complications with Sample Vetting Criteria

It is interesting to note that despite the screening criteria, vetting samples eliminated little scatter. In fact, the data screening process removed a relatively homogeneous set of data from the strontium curve. The perturbations at 534.3 Ma and 529.6 Ma, for instance, are not screened from the data. It is possible that these data are genuine signals recorded in the rock record; however, it is also possible that the traditional screening mechanisms for strontium isotopes are not applicable in the early Cambrian due to the abnormal seawater chemistry.

The traditional vetting criteria are based on the rough negative correlation between Sr and Mn in recrystallized carbonates (Brand and Veizer, 1980). The three major assumptions that underlie this screening technique are: (1) that shallow marine carbonates are precipitated in seawater with lower Sr/Ca, Mg/Ca, and Na/Ca than average seawater, (2) that shallow marine carbonates are precipitated in seawater with higher Mn/Ca and Fe/Ca, and (3) that changes in these systems are connected and predictable (Nicholas, 1996). These underlying assumptions are effective for strontium isotopes collected through analysis of animal tests and shells as well as preserved primary carbonates deposited in modern oceans with modern redox conditions. However, redox conditions during the Cambrian varied greatly from modern redox conditions (Fike et al., 2006), and changes of redox-controlled metal deposition complicates this system (Nicholas, 1996). In particular, precipitation of iron oxyhydroxide and manganese oxides at near-surface carbonates (carbonate deposits near the seawater-sediment boundary) creates faux enrichment of these elements in major-element screening techniques (Weiss & Wilkinson, 1988). If strontium enrichment through meteoric waters is the cause of elevated Mn and Fe values, as has been suggested in prior studies (Kaufman, 1993; Nicholas, 1996), then a positive correlation between strontium isotope values and

[Mn] and [Fe] should be present. As illustrated in Figure 11, we see no correlation between elevated 87Sr inputs and increased [Mn] and [Fe].

If the transition from aragonite to calcite seas is driven by an increase in deep water temperature, then an effective source of calcium and sink for magnesium is responsible for driving the change in dominant seawater cations. It is tricky to determine the fate of strontium ions during such a change. However, if the transition is instead driven by dolomitzation, strontium is released back into the seawater. Thus, the dolomitization acts as a potential third source of strontium (the other two being mid ocean ridges and continental weathering).

Additionally, the changing seawater chemistry changes many of the chemical signatures traditionally used to screen strontium isotope data. Due to this great uncertainty pertaining to ocean chemistry during the early Cambrian (changing Mg/Ca ratios, unknown residence time of Sr, changing Sr reservoir size, unknown clay deposition in deep oceans, unknown mid-ocean ridge spreading rate, unknown redox state of lower oceans, etc.) traditional vetting criteria are suspect. Thus, we present the majority of our data for consideration, and have removed only samples with visible diagenesis or low carbonate concentrations.

Samples that did not pass the vetting criteria were examined individually. These samples were predominantly from the upper half of the stratigraphy, and are included despite low strontium concentrations as there is little evidence of alteration. For instance, some samples taken from the upper Bayangol and lower Salaagol formations were included in the final data set despite low concentrations of total strontium. Because these data span the transition from aragonitic to calcitic seas, it is inferred that the ocean chemistry undergoes changes, and total strontium content of the basin may experience a shift during this time. The decreased concentrations of strontium in the upper stratigraphy may reflect this global transition from aragonite to calcite seas during the early Cambrian (strontium fits more readily into an aragonite matrix as magnesium is a larger ion than calcium).

Seawater chemistry throughout the Precambrian/Cambrian transition period has a drastically different signal from modern ocean chemistry with different oxidation states (Fike et al., 2006) and changing phosphate concentrations (Planavsky, 2010).

Many of the samples which did not pass traditional Phanerozoic strontium isotope screening cutoffs show no evidence of additional diagenesis, have low rubidium concentrations, high strontium concentrations, and are >90% carbonate. Therefore, we present all data with >90% carbonate in the strontium isotope curve used in this discussion and interpretation and do not distinguish between samples with high Mn, Fe, or Mg concentration. Moreover, lithological constraints in the measured sections indicate multiple transgressive and regressive cycles in the sequence (Smith et al., in review). This cyclic sequence stratigraphy in the basin suggests that the basin was restricted and opened several times. As the foreland basin is restricted, local weathering fluxes provide a relatively larger role in determining the strontium isotope signature. It is possible that changing reservoir size changes the seawater chemistry system and complicates these vetting criteria.

Constructing a New Global Composite Strontium Isotope Curve

To compare our data with previously measured strontium isotope ratios throughout the early Cambrian, we compare the newly refined Mongolian age model. Our age model adjusted the dates of previously plotted data from Mongolia (see discussion for further detail). The composite data curve is taken from eight locations world-wide (Figure 14).

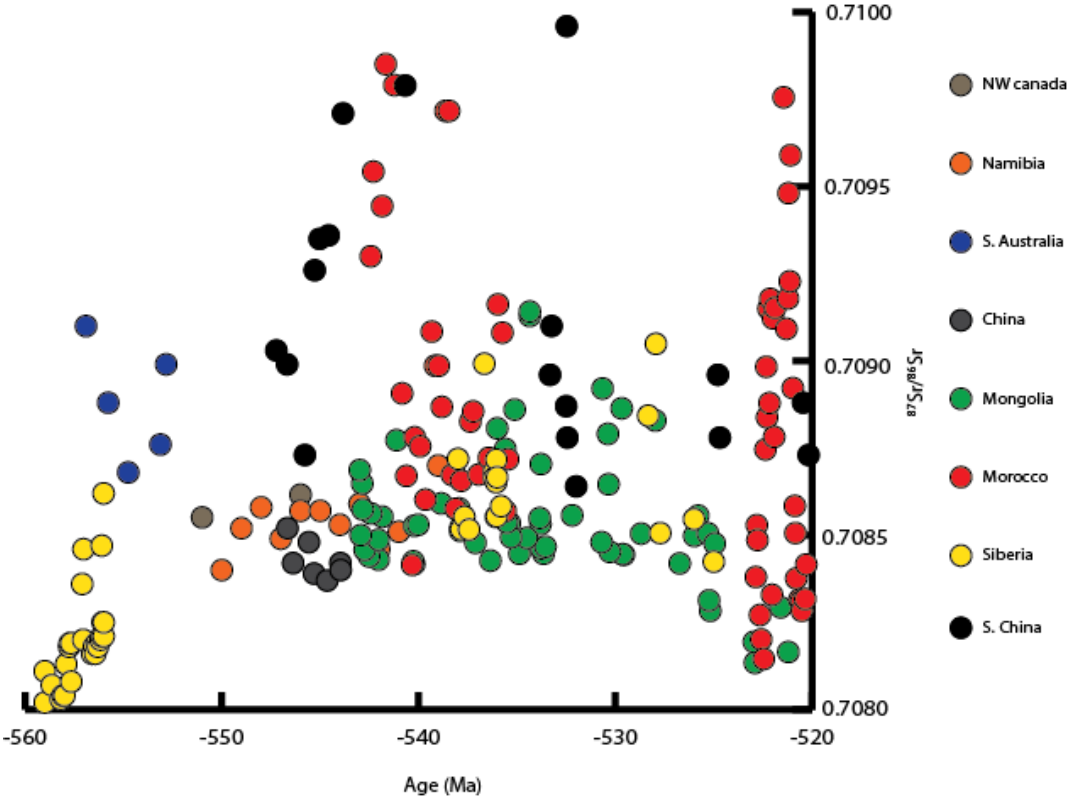

Figure 13. Composite strontium isotope curve from the late Ediacaran through the early Cambrian. Note the initial rise in strontium (~560 Ma, Siberia data) correlated with the collapse of the Pan-African Orogeny and the long stable period between 550-530 Ma. Data sources from Halverson et al., 2007 and Rooney et al., 2014 (NW Canada); Halverson et al., 2007 and Kaufmann et al., 1993 (Namibia); Calver, 2000 (Australia); Sawaki et al., 2010 (China); Maloof et al., 2010 (Morocco); Melezhik et al, 2009, Derry et al., 1994, Nicholas, 1996 and Vinogradov et al, 1996 (Siberia); Shields et al., 2002, Brasier et al., 1996, and this study (Mongolia); Ishikawa et al., 2008 (S. China).

The decrease in strontium isotopes around 522 Ma has previously been interpreted as a long-term downward trend (Maloof et al., 2010). Maloof et al., 2010 propose that this decrease in strontium isotopes is the result of a 2.5x increase in mid-ocean ridge spreading rates. However, as the new data indicate a stable strontium isotope value through 522 Ma, the downward trend in strontium isotope

values appears sudden. It is interesting to note that this rapid decline in strontium isotope values is coincident with the convergence of magmatic arcs in Antarctic sequences (Encarnacion & Grunow, 1996; Vogel et al., 2002) and the formation of mafic-ultramafic complexes preserved in Tasmania interpreted as part of the Terra Australis orogeny at 520 Ma (Brown et al., 1986; Cawood, 2005). These complexes may increase the relative concentration of a mantle signal in the strontium isotope curve due to a change in the composition of weathered material.

New preliminary data indicates that this downward trend may be more protracted than is evident in Figure 14 (Appendix A).

Increased Weathering in the early Cambrian?

Increased continental weathering transports additional nutrient fluxes to the oceans (Derry et al., 1994) and the formation of the Great Unconformity has been suggested to increase shallow sea habitat (Peters and Gaines, 2012), potentially fueling the explosion of life during this time period. Increased hydrothermal activity and mid-ocean ridge spreading could also potentially have a cascade effect on the biologic potential of ocean systems. A tectonic reorganization of the continents can also affect ocean circulation patterns, nutrient concentrations and dispersal, and the formation of extensive shallow seas (Tucker, 1992). Bursts in hydrothermal activity have been linked with anoxia, high organic carbon burial, and phosphogenesis (Jenkyns 1980; Compton et al., 1996). Sediments from the early Cambrian have preserved notable carbon isotope excursions, phosphatic horizons, and redox-sensitive sediments, which would all be expected from this proposed increase in tectonic activity in the early Cambrian (Porada, 1989; Derry et al., 1994). Again, the evidence from the sedimentology can be interpreted in the context of a proposed increased hydrothermal and tectonic activity, and yet, the

main evidence presented for this driver is the Ediacaran to Cambrian strontium isotope record.

Numerous processes have been proposed to account for increased weathering in the early Cambrian including sea level rise (Dalziel et al, 2014), the breakdown of the Pan-African orogeny (Derry et al., 1994), and the formation of the Great Unconformity (Peters and Gaines, 2012). These proposed weathering increases suggest that a significant increase in sediment input into ancient oceans may increase shallow sea habitat and change the nutrient chemistry in the ocean (Peters and Gaines, 2012; Dalziel et al., 2014). Such changes may in turn be responsible for many of the unique chemical signals of the early Cambrian. A drastic increase in weathering is expected to leave a strontium isotope fingerprint of elevated $^{87}Sr/^{86}Sr$ ratios due to the increased continental inputs. However, our data indicate stable relative weathering to hydrothermal activity through the early Cambrian. It could be possible for large volumes of material to shed off continents into the ocean without altering the strontium isotope record, however, such a signal would require another system input (i.e. equally large increase in mid-ocean ridge spreading). It is unlikely that such a change would be synchronous and not leave large perturbations in the strontium record. Our results and the compilation curve do not indicate elevated $^{87}Sr/^{86}Sr$ ratios through the 550-525 Ma time interval.

Increased Mid-Ocean Ridge Activity in the early Cambrian?

Contrary to the proposed weathering-based sources of strontium through the early Cambrian, which would be expected to record an increase in strontium isotopes through the early Cambrian, proposed increases in seafloor spreading and volcanism during the early Cambrian are expected record a decrease in $^{87}Sr/^{86}Sr$ isotope ratios. The composite strontium isotope curve (Maloof et al., 2010) is interpreted to record this decrease in $^{87}Sr/^{86}Sr$ that is interpreted to be consistent

with a 2.5 fold increase in mid-ocean ridge spreading rates. However, the Maloof et al. data is limited by two factors: (1) a reliance on an age correlation between models, which we refine in our interpretation and (2) immense data scatter. The data have previously been interpreted by creating a generic age model and following the lowest $^{87}Sr/^{86}Sr$ trend. New age correlations connecting our data to the Brasier, 1996 Mongolia data indicate that certain age model correlations in this composite data set are inaccurate. Data presented in this paper show no change in strontium isotope values over this time period and is therefore inconsistent with this model.

The 2.5 fold increase in mid-ocean ridge spreading rate is also a proposed mechanism driving the change from aragonitic to calcitic seas and carbon isotope variations (Maloof et al., 2010).

Confounding Factors

The transition from magnesium to calcium dominated seawater chemistry is intimately linked to the strontium cycle. As previously mentioned, strontium isotopes are traditionally vetted on concentration of strontium, magnesium, rubidium, iron, manganese, carbonate content, and diagenetic indicators (Kaufman et al., 1993; Nicholas et al., 1993; Moore 1989). The use of these screening criteria, however, assumes constant and known seawater chemistry compositions. During the early Cambrian, the transition from aragonite to calcite seas and the corresponding transition from excess Mg^{2+} ions to Ca^{2+} cations (Sandberg, 1983) is likely to have numerous effects on the overall chemical composition of seawater which, in turn, alters the screening criteria for strontium isotopes. There are several proposed mechanisms for this transition from aragonite to calcite seas including an increase of high temperature alteration of carbonate muds in the deep ocean and a large-scale dolomitization front (Holland and Zimmermann, 2000; Hardie, 1996).

The effects of these hypothesized changes in seawater chemistry on strontium isotope preservation and interpretation are discussed in the following two sections.

Dolomitization Fronts as Mg Sink and Sr Source

During dolomitization, pore fluid mixing enables magnesium ions to replace calcium ions in the carbonate lattice, causing a 13% volume reduction (Landes, 1946) and the release of up to 90% of the strontium contained in the original carbonate back into the seawater (James et al., 2005). The early Cambrian Period was likely dominated by primarily aragonite deposition therefore carbonates had high Mg concentrations (Porter, 2007). Carbonates with high Mg concentrations incorporate between 5-9 times more strontium into their lattice structure during deposition than low Mg carbonates due to the thermodynamic stability of replacing a large Mg ion with a Sr ion as compared with the thermodynamic instability of replacing a small Ca cation with a large Sr ion (Swart et al., 2001).

One proposed mechanism driving the transition from Mg to Ca dominated seawater is an increase in dolomitization (Folk, 1965; Katz et al., 1973). Increased relative sea level in the early Cambrian (Haq and Chutter, 2008) after the rift of Rodinia and subsidence of many margins may have increased the volume of submerged carbonate platforms, further increasing the effect of a large-scale dolomitization front on seawater chemistry. The increased dolomitization would act as a sink for Mg ions; however, this conversion of aragonite to calcite changes both the isotope budget and concentration within a fully mixed ocean (Stoll and Schrag, 1998). If, indeed such an increase in global dolomitization occurred, it is possible that much of the strontium isotope record through the early Cambrian is the result of recycled Sr ions released back into the ocean system during dolomitization. This rapid increase in the strontium reservoir would influence

residence time, concentration in carbonates, and isotope ratios of strontium isotopes. It is possible that the flat-line strontium isotope curve presented here is the result of recycled strontium ions from broad-scale dolomitization.

A few major assumptions must be made to estimate the order of magnitude impact dolomitization may have on the strontium inputs. Peters and Gaines estimate that in the early Cambrian, ~100,000 km^3 of carbonates are deposited every million years in Laurentia (Peters and Gaines, 2012). As Laurentia represents roughly 33% of the land-mass near the equator in the early Cambrian, a rough guess for total carbonate production is ~350,000 km^3. Of these deposited carbonates, it is estimated that 48% will be dolomitized (estimate based on percent dolomite in preserved sediments from early Cambrian) (Vinogradov & Ronov, 1956). An average value of ~500 ppm Sr was taken from major elements data used in this study. The density of $CaCO_3$ was taken to be 2.71 g/cm^3.

Let the following variables be defined:

α = fraction of carbonates dolomitized

β = fraction of Sr released from carbonates during dolomitization

γ = concentration of strontium in deposited carbonates

ρ = density of carbonates

V = carbonate volume

t = time

$$\left(\frac{V}{t}\right)\rho\alpha\gamma\beta = \frac{recycled\ Sr\ weight}{time}$$

$$\frac{3.5x10^{20}cm^3}{My} * \frac{2.71g}{cm^3} * (0.48) * (500ppm) * (0.85) = \frac{\mathbf{1.93x10^{20}\ mg\ Sr}}{\mathbf{My}}$$

So the flux of recycled strontium from dolomitization is estimated to be $1.93x10^{20}$ mg/My, or $1.93x10^{8}$ kg/yr. Given that the average strontium flux from

mid ocean ridges is estimated to be on the order of $1.2x10^{14}$ kg/yr (Palmer & Edmond, 1989), it seems unlikely that the stable strontium trend through the early Cambrian is due entirely to dolomitization.

High and Low Temperature Carbonatization

The transition from aragonite to calcite seas in the early Cambrian has also been attributed to an increase in spreading rates (Hardie, 1996; Maloof, 2010). Exchange of Mg on the seafloor can be attributed to one of two processes: an increase in hydrothermal activity (specifically mid-ocean ridge spreading), or an increase in bottom water temperature that results in increased Mg-rich clay deposition. To drive the transition from aragonite to calcite seas through mid-ocean ridge spreading, a 2.5 fold spreading rate increase would be required (Maloof et al., 2010). Such a large increase in mid ocean ridge spreading would likely still dominate the strontium isotope system (to accommodate a 2.5 fold increase in mid ocean ridge spreading, strontium isotopes would be expected to drop by a factor of 0.0006) (Maloof et al., 2010). The homogeneity of strontium isotopes in the early Cambrian presented here is difficult to explain in a paleo-environment with rapidly increasing spreading rates.

However, it is possible that the transition from aragonite to calcite seas was driven by increased bottom water temperatures caused by a global climate change, rather than a geophysical change. Cold deep water temperatures limit magnesium exchange in carbonates and may manifest itself in a decreased residence time for strontium. For instance, rapid, cyclic sea level changes in early Cambrian sediments (Smith et al., in review) are difficult to accommodate without the presence of ice in the early Cambrian environment (Bertrand-Safari et al., 1995; Trompette, 1996; Harland, 1983). A long warming trend in the early Cambrian may have the capacity to warm deep ocean temperatures sufficiently enough to alter mud composition.

Implications of a Mg to Ca Transition on Sr Residence Time

Regardless of the driving mechanism, the transition from aragonite to calcite seas in the early Cambrian will impact the strontium reservoir. As high Mg carbonates (i.e. aragonite) take up between 5-9 times more strontium into their lattice structure during deposition than low Mg carbonates (Swart et al., 2001), the strontium reservoir after the transition to calcite seas should be much higher than the strontium reservoir during times of aragonite precipitation. The impact of changing the strontium reservoir is two-fold: (1) the co-precipitation model indicates that altering the ratio of a trace element in the surrounding environment to the concentration of the major element which it replaces will alter the concentration of trace element growth in crystals (Doerner and Hoskins, 1925); and, (2) residence time of strontium in oceans will change. These two changes result in a strontium cycle that is less susceptible to small changes in source fluxes. The modern oceans (calcite dominated) have a strontium residence time of approximately two million years (Veizer et al., 1989). However, prior to the transition to calcite seas, this residence time was likely much higher and strontium ion concentration was more susceptible to slight environmental changes due to decreased strontium reservoir size. It is difficult to determine the impacts of changing reservoir size on the stability of strontium isotopes, but it is important to note that perhaps some of the stability of the early Cambrian strontium isotope curve can be attributed to the sudden increase in strontium reservoir size.

The transition from calcite to aragonite seas manifests itself in the strontium cycle in both the residence time and the size of the stable strontium reservoir in the ocean. The changes in residence time and reservoir size can be calculated by modeling the strontium residence time for calcite seas as a function of the mass of strontium in the ocean, the flux of strontium into the ocean, and the flux of

strontium out of the ocean. There strontium flux into the ocean is modeled with three sources: riverine fluxes, calcium carbonate dissolution, and hydrothermal venting. This study used approximate values from Palmer and Edmond, 1989 and Hodell et al., 1990.

$\Phi_{riverine} = 33.3x10^9$ mol/yr

$\Phi_{CaCO3} = 3.4x10^9$ mol/yr

$\Phi_{hydrothermal} = 14.4x10^9$ mol/yr

$\Phi_{in} = \Phi_{riverine} + \Phi_{CaCO3} + \Phi_{hydrothermal} = 51.1x10^9$ mol/yr

Flux out of the ocean system is predominantly driven by strontium incorporation into carbonate lattices. The flux of strontium out of the ocean into precipitated carbonate can be calculated by determining rate of carbonate deposition and concentration of strontium in deposited carbonates.

γ = concentration of strontium in deposited carbonates = 500 ppm

ρ = density of carbonates = 2.71 g/cm^3

$\left(\frac{V}{t}\right)$ = carbonate volume/time = $3.5x10^{20}$ cm^3/My

$\Phi_{out} = \gamma\rho\left(\frac{V}{t}\right) = 5.41x10^9$ mol/yr

If we assume that the ocean/strontium system is in steady state, then the residence time (τ) of strontium in the ocean can be estimated as $\frac{\text{mass of Sr in ocean}}{\Phi_{in}-\Phi_{out}}$. Mass of strontium in the ocean is estimated at $1.25x10^{17}$mol (Hodell et al., 1990).

$\tau = \frac{1.25x10^{17}\text{mol}}{51.1x10^9\text{mol/yr}-5.41x10^9\text{mol/yr}} = 2.7x10^6$ years

To accommodate the change in strontium uptake with the transition from aragonite to calcite seas, the flux out is multiplied by a factor of eight due to the

change in accommodation of strontium into lattice structures (Veizer et al., 1989). Thus in aragonite seas, the $\Phi_{out\_aragonite}$ is approximated to be $4.33x10^{10}$ mol/yr.

Along with the Φ_{out}, both the residence time and the reservoir volume will change. The minimum strontium reservoir in an aragonite sea can be estimated by holding the residence time constant, but changing Φ_{out} to $\Phi_{out\_aragonite}$.

$$\tau = \frac{\text{Min Sr Reservoir}}{51.1x10^{9}\text{mol/yr} - 4.33x10^{10}\text{mol/yr}} = 2.7x10^{6} \text{ years}$$

Minimum Sr Reservoir with aragonite seas = $2.11x10^{16}$ mol.

Likewise the maximum change in strontium residence time can be calculated by holding the reservoir size constant.

$$\tau = \frac{1.25x10^{17}\text{mol}}{51.1x10^{9}\text{mol/yr} - 4.33x10^{10}\text{mol/yr}} = 16.0x10^{6} \text{ years}$$

These results are summarized in Table 1.

	Calcite Seas	Aragonite Seas
Reservoir Size (mol Sr)	$1.25x10^{17}$	$2.11x10^{16}$ (min)
Residence Time (years)	$2.5x10^{6}$	$16x10^{6}$ (max)
Flux Out (mol/year)	$5.41x10^{9}$	$43.3x10^{9}$

Table 1. Results of modeled changes in reservoir size, residence time, and flux out for calcite and aragonite seas. As incorporating a strontium ion into a high-magnesium carbonate lattice is thermodynamically more favorable than incorporating a strontium into a low-magnesium carbonate lattice, aragonite seas have smaller reservoir size and longer residence times for strontium ions.

The residence time and reservoir size of strontium in an aragonite sea would change by a maximum factor of ~6. Thus the strontium reservoir may have been susceptible to larger excursions from smaller changes in flux during the aragonite sea period.

Understanding the "Cambrian Explosion"

Many of the proposed hypotheses for trigger mechanisms for the Cambrian explosion have called on environmental changes (Maloof et al., 2010; Peters and Gaines 2012; Dalziel 2014). Current hypotheses which may be recorded in the strontium isotope record include: (1) drastic transgressions (sea level rises) that increased habitat and altered ocean chemistry (Dalziel et al, 2014); (2) weathering inputs from the Transgondwanan Supermountain increased nutrient inputs to the ocean system (Squire et al., 2006); (3) Seafloor spreading rate increased by a factor of 2.5 which was linked to an ocean chemistry change (Maloof et al., 2010); and (4) the massive weathering event which eventually resulted in the Great Unconformity shed nutrients into the oceans and increased habitat for shallow marine life forms to expand (Peters and Gaines, 2012). Any of these drastic changes in the environmental systems are likely to shock the strontium system. The data presented herein is inconsistent with all of the models presented above. These data challenge interpretations that relate tectonic drivers and environmental change to the Cambrian explosion. Perhaps, rather than an environmental change triggering notable changes in biology, evolution of biologic changes lead to drastic changes in the environmental system.

CONCLUSIONS

We present an additional strontium isotope curve through the early Cambrian period to add resolution to a curve prone to large scatter, contradicting interpretations, and secondary alteration. These data provide insight into the environmental conditions in the early Cambrian, an era the rock record indicates to be in a state of flux. Our strontium isotope curve through the early Cambrian indicates a stable, non-trending ratio of $^{87}Sr/^{86}Sr$. This period of relative stability is notable as it is sandwiched between the drastic global signal of the Pan-African Orogeny and the beginning of a long decreasing trend through the late Cambrian and Ordovician. Prior interpretations for the strontium isotope of the early Cambrian have included both a general increase in strontium isotope values through the early Cambrian as well as a long-term decrease in values. We present data that indicate a relatively stable strontium isotope ratio between 0.7085 and 0.7090 throughout this time period.

These data do not support hypotheses indicating drastic environmental changes through the early Cambrian (i.e. 2.5 fold increase in mid-ocean ridge spreading, large-scale global continental denudation, etc.). However, interpretations of these data are confounded by the complexities of the strontium isotope system as well as the changing ocean chemical composition during the early Cambrian period. The strontium isotope curve is influenced by changing Mg and Ca budgets as well as deep ocean chemical changes, none of which are well constrained through the early Cambrian.

APPENDIX A: Isotope values for samples with %carbonate > 85%

Sample	$^{87}Sr/^{86}Sr$ corrected	Age
E1129-106	0.708454111	
E1129-155	0.708485398	
E1129-20.5	0.708476797	
E1129-66	0.70845321	
E1138-177	0.708509244	537.0133333
E1138-228	0.708714711	536.0355556
E1207-285	0.708551959	
E1207-292	0.708599635	
E1211-506	0.708604964	534.8448276
E1211-565	0.708516007	534.5057471
E1211-589	0.708494507	534.3678161
E1216-35	0.708554403	542
E1216-66	0.708555467	542.1
E1220-109	0.708591317	538.8513514
E1220-139	0.708576788	537.9391892
E1220-146	0.708512573	537.8918919
E1220-151	0.708523971	537.8581081
E1220_154	0.708628041	537.8378378
E1220_430	0.708769075	535.9876645
E1220-432	0.708806493	536.0049335
E1220_434	0.708830812	535.95
E1220_440	0.708726559	535.9
E1220-445	0.708552196	536.0690771
E1220-556	0.708533841	535.3634868
E1220-602	0.708860348	535.1167763
E1220-743	0.709129011	534.3478261
E1220-743	0.709141277	534.3478261
E1220_760	0.708416745	534.1488294
E1220_792	0.708703826	533.7859532
E1220-803	0.708446771	533.6454849
E1220-889	0.708531557	533.8094
E1220-892	0.708549077	533.8444782
E1220_927	0.708556966	532.1939799
E1220-980	0.708446771	534.8745734

E1220_993	0.708379077	531.3862876
E1220_1072	0.708645859	530.3465046
E1220-1117	0.708863905	529.6778116
E1220-1148.5	0.708443865	529.56383
E1220-1153	0.708445471	529.63222
E1120_1174	0.708156143	528.7203647
E1220-1187	0.70850446	528.6899696
E1220-1310	0.708419192	526.7294833
E1220-1360	0.708497968	525.990566
E1220-1400	0.70855621	525.7924528
E1220-1507	0.708505225	525.3018868

Table 1. All data points with %carbonate > 85%.

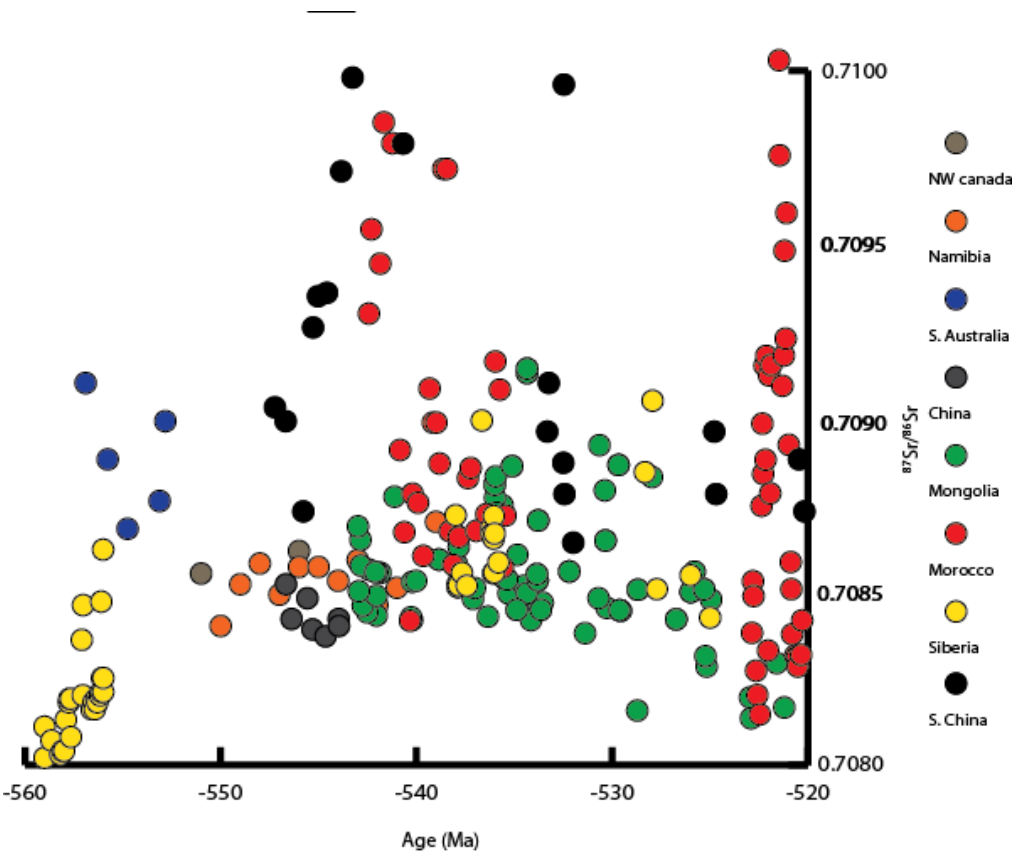

Figure 1. Global strontium curve with all data. Note that there are an additional 10 preliminary data points incorporated into this data set. The low outlier ~529 Ma may indicate a more protracted decline in strontium isotopes at the end of the

studied time interval than the data otherwise indicates. However, these data require further investigation.

WORKS CITED

Badarch, G., Cunningham, W. D., & Windley, B. F. (2002). A new terrane subdivision for Mongolia: implications for the Phanerozoic crustal growth of Central Asia. Journal of Asian Earth Sciences, 21(1), 87-110.

Bertrand-Sarfati, J., Moussine-Pouchkine, A., Amard, B., & Ahmed, A. A. K. (1995). First Ediacaran fauna found in western Africa and evidence for an Early Cambrian glaciation. Geology 23(2), 133-136.

Bezzubtsev, V.V., 1963, On the Precambrian-Cambrian stratigraphy of the Dzabkhan River Basin: Materials on the Geology of MPR, Gostopotekhizdat, p. 29-42.

Brand, U., & Veizer, J. (1981). Chemical diagenesis of a multicomponent carbonate system-2: stable isotopes. Journal of Sedimentary Research, 51(3).

Bold, U., Macdonald, F.A., Smith, E.F., Crowly, J.C., Minjin, C., Dorjnamjaa.D., 2013. Elevating the Neoproterozoic Tsagaan-Olom Formation to a Group. Mongolian Geoscientist 39, 5.

Brasier, M. (1982). Sea-level changes, facies changes and the Late Precambrian—Early Cambrian evolutionary explosion. Precambrian Research, 17(2), 105-123.

Brasier, M. (1992). Background to the Cambrian explosion. Journal of the Geological Society, 149(4), 585-587.

Brasier, M., Shields, G., Kuleshov, V., & Zhegallo, E. (1996). Integrated chemo- and biostratigraphic calibration of early animal evolution: Neoproterozoic–early Cambrian of southwest Mongolia. Geological Magazine, 133(04), 445-485.

Brasier, M. D. (1996). The basal Cambrian transition and Cambrian bio-events (from terminal Proterozoic extinctions to Cambrian biomeres) Global events and event stratigraphy in the Phanerozoic (pp. 113-138): Springer.

Brass, G. W. (1976). The variation of the marine 87Sr86Sr ratio during Phanerozonic time: interpretation using a flux model. Geochimica et Cosmochimica Acta, 40(7), 721-730.

Broecker, W. S. (1963). Radioisotopes and large-scale oceanic mixing. The sea, 2, 88-108.

Brown, A.V., 1986. Geology of the Dundas-Mount Lindsay-Mount Youngbuck Region, Bulletin 62. Geological Survey of Tasmania, Hobart, 221 pp.

Burke, W., Denison, R., Hetherington, E., Koepnick, R., Nelson, H., & Otto, J. (1982). Variation of seawater 87Sr/86Sr throughout Phanerozoic time. Geology, 10(10), 516-519.

Calver, C. R. (2000). Isotope stratigraphy of the Ediacarian (Neoproterozoic III) of the Adelaide Rift Complex, Australia, and the overprint of water column stratification. Precambrian Research, 100(1), 121-150.
Cawood, P. A. (2005). Terra Australis Orogen: Rodinia breakup and development of the Pacific and Iapetus margins of Gondwana during the Neoproterozoic and Paleozoic. Earth-Science Reviews, 69(3), 249-279.
Compton, J. S., & Mallinson, D. J. (1996). Geochemical consequences of increased late Cenozoic weathering rates and the global CO2 balance since 100 Ma. Paleoceanography, 11(4), 431-446.
Cook, P., & Shergold, J. (1986). Proterozoic and Cambrian phosphorites-nature and origin. Phosphate deposits of the world, 1, 369-386.
Corsetti, F.A., and Hagadorn, J.W., 2000, Precambrian-Cambrian transition: Death Valley, United States: Geology, v. 28, no. 4, p. 299-302.
Davis, D., Gray, J., Gumming, G., & Baadsgaard, H. (1977). Determination of the 87 Rb decay constant. Geochimica et Cosmochimica Acta, 41(12), 1745-1749.
Dalziel, I. W. (2014). Cambrian transgression and radiation linked to an Iapetus-Pacific oceanic connection?. Geology, 42(11), 979-982.
DePaolo, D. J., & Ingram, B. L. (1985). High-resolution stratigraphy with strontium isotopes. Science, 227(4689), 938-941.
Derry, L., Brasier, M., Corfield, R. e. a., Rozanov, A. Y., & Zhuravlev, A. Y. (1994). Sr and C isotopes in Lower Cambrian carbonates from the Siberian craton: a paleoenvironmental record during the 'Cambrian explosion'. Earth and Planetary Science Letters, 128(3), 671-681.
Doerner, H., & Hoskins, W. M. (1925). Co-precipitation of Radium and Barium Sulfates. Journal of the American Chemical Society, 47(3), 662-675.
Dorjnamjaa, D., & Bat-Ireedui, Y.(1991). The Precambrian of Mongolia: Ulaanbaatar: Geological Institute of the Mongolian Academy of Sciences.
Edmond, J. (1992). Himalayan tectonics, weathering processes, and the strontium isotope record in marine limestones. Science-New York then Washington, 258, 1594-1594.
Encarnación, J. and Grunow, A., 1996. Changing magmatic and tectonic styles along the paleo-Pacific of Gondwana and the onset of early Paleozoic magmatism in Antarctica. Tectonics, 15: 1325-1341.
Farrell, J. W., Clemens, S. C., & Gromet, L. P. (1995). Improved chronostratigraphic reference curve of late Neogene seawater 87Sr/86Sr. Geology, 23(5), 403-406.
Fike, D., Grotzinger, J., Pratt, L., & Summons, R. (2006). Oxidation of the Ediacaran Ocean. Nature, 444(7120), 744-747.
Folk, R. L. (1965). Some aspects of recrystallization in ancient limestones. The Society of Economic Paleontologists and Mineralogists. 14-48.

Fritz, P., & Katz, A. (1972). The sodium distribution of dolomite crystals. Chemical Geology, 10(3), 237-244.
Gibsher, A., and Khomentovsky, V., 1990, The section of the Tsagaan Oloom and Bayan Gol Formations of the Vendian–Lower Cambrian in the Dzabkhan zone of Mongolia: The Late Precambrian and Early Paleozoic of Siberia. Institut Geologii I Geofiziki, Sibirskoe Otdelenie, Akademiya Nauk SSSR, Novosibirsk, p. 79-91.
Gibsher, A., Bat-Ireeduy, Y., Balakhonov, I., Efremenko, D., & Khomentovsky, V. (1991). Bayangol reference section, Vendian-Lower Cambrian central Mongolia: divisions and correlation. The late Precambrian and early Palaeozoic of Siberia: The Siberian platform and its framework, 107-120.
Gibson, T., Myrow, P., Macdonald, F., Minjin, C., & Gehrels, G. (2013). Depositional history, tectonics, and detrital zircon geochronology of Ordovician and Devonian strata in southwestern Mongolia. Geological Society of America Bulletin, 125(5-6), 877-893.
Goldring, R., & Jensen, S. (1996). Trace fossils and biofabrics at the Precambrian–Cambrian boundary interval in western Mongolia. Geological Magazine, 133(04), 403-415.
Halverson, G. P., Dudás, F. Ö., Maloof, A. C., & Bowring, S. A. (2007). Evolution of the 87 Sr/86 Sr composition of Neoproterozoic seawater. Palaeogeography, Palaeoclimatology, Palaeoecology, 256(3), 103-129.
Haq, B. U., & Schutter, S. R. (2008). A chronology of Paleozoic sea-level changes. Science, 322(5898), 64-68.
Hardie, L. A. (1996). Secular variation in seawater chemistry: An explanation for the coupled secular variation in the mineralogies of marine limestones and potash evaporites over the past 600 my. Geology, 24(3), 279-283.
Harland, W. B. (1983). The Proterozoic glacial record. Geological Society of America Memoirs, 161, 279-288.
Hodell, D. A., Mead, G. A., & Mueller, P. A. (1990). Variation in the strontium isotopic composition of seawater (8 Ma to present): Implications for chemical weathering rates and dissolved fluxes to the oceans. Chemical Geology: Isotope Geoscience section, 80(4), 291-307.
Holland, H. D., & Zimmermann, H. (2000). The Dolomite Problem Revisited1. International Geology Review, 42(6), 481-490.
Ishikawa, T., Ueno, Y., Komiya, T., Sawaki, Y., Han, J., Shu, D., ... & Yoshida, N. (2008). Carbon isotope chemostratigraphy of a Precambrian/Cambrian boundary section in the Three Gorge area, South China: prominent global-scale isotope excursions just before the Cambrian Explosion. Gondwana Research, 14(1), 193-208.
James, N. P., & Klappa, C. F. (1983). Petrogenesis of early Cambrian reef limestones, Labrador, Canada. Journal of Sedimentary Research, 53(4).

Jenkins, W., Rona, P., & Edmond, J. (1980). Excess 3 He in the deep water over the mid-Atlantic ridge at 26 N: evidence of hydrothermal activity. Earth and Planetary Science Letters, 49(1), 39-44.

Jones, C. E., Jenkyns, H. C., Coe, A. L., & Stephen, H. P. (1994). Strontium isotopic variations in Jurassic and Cretaceous seawater. Geochimica et Cosmochimica Acta, 58(14), 3061-3074.

Katz, A. (1973). The interaction of magnesium with calcite during crystal growth at 25–90 C and one atmosphere. Geochimica et Cosmochimica Acta, 37(6), 1563-1586.

Kaufman, A. J., Jacobsen, S. B., & Knoll, A. H. (1993). The Vendian record of Sr and C isotopic variations in seawater: implications for tectonics and paleoclimate. Earth and Planetary Science Letters, 120(3), 409-430.

Kaufman, A. J., & Knoll, A. H. (1995). Neoproterozoic variations in the C-isotopic composition of seawater: stratigraphic and biogeochemical implications. Precambrian Research, 73(1), 27-49.

Kaufman, A. J., Knoll, A. H., Semikhatov, M. A., Grotzinger, J. P., Jacobsen, S. B., & Adams, W. (1996). Integrated chronostratigraphy of Proterozoic–Cambrian boundary beds in the western Anabar region, northern Siberia. Geological Magazine, 133(05), 509-533.

Khomentovsky, V., & Gibsher, A. (1996). The Neoproterozoic–lower Cambrian in northern Govi-Altay, western Mongolia: regional setting, lithostratigraphy and biostratigraphy. Geological Magazine, 133(04), 371-390.

Kirschvink, J. L., Ripperdan, R. L., & Evans, D. A. (1997). Evidence for a large-scale reorganization of Early Cambrian continental masses by inertial interchange true polar wander. Science, 277(5325), 541-545.

Knoll, A. H., & Carroll, S. B. (1999). Early animal evolution: emerging views from comparative biology and geology. Science, 284(5423), 2129-2137.

Knoll, A. H., Kaufman, A. J., & Semikhatov, M. A. (1995). The carbon-isotopic composition of Proterozoic carbonates: Riphean successions from northwestern Siberia (Anabar Massif, Turukhansk Uplift). American Journal of Science, 295(7), 823-850.

Kouchinsky, A., Bengtson, S., Pavlov, V., Runnegar, B., Torssander, P., Young, E., & Ziegler, K. (2007). Carbon isotope stratigraphy of the Precambrian–Cambrian Sukharikha River section, northwestern Siberian platform. Geological Magazine, 144(04), 609-618.

Kröner, A., Lehmann, J., Schulmann, K., Demoux, A., Lexa, O., Tomurhuu, D., Wingate, M. T. (2010). Lithostratigraphic and geochronological constraints on the evolution of the Central Asian Orogenic Belt in SW Mongolia: Early Paleozoic rifting followed by late Paleozoic accretion. American Journal of Science, 310(7), 523-574.

Kruse, P. D., Gandin, A., Debrenne, F., & Wood, R. (1996). Early Cambrian bioconstructions in the Zavkhan Basin of western Mongolia. Geological Magazine, 133(04), 429-444.

Kump, L. R., & Arthur, M. A. (1999). Interpreting carbon-isotope excursions: carbonates and organic matter. Chemical Geology, 161(1), 181-198.

Landes, K. K. (1946). Porosity through dolomitization. AAPG Bulletin, 30(3), 305-318.

Lehmann, J., Schulmann, K., Lexa, O., Corsini, M., Kröner, A., Štípská, P., Otgonbator, D. (2010). Structural constraints on the evolution of the Central Asian Orogenic Belt in SW Mongolia. American Journal of Science, 310(7), 575-628.

Lindsay, J., Brasier, M., Dorjnamjaa, D., Goldring, R., Kruse, P., & Wood, R. (1996). Facies and sequence controls on the appearance of the Cambrian biota in southwestern Mongolia: implications for the Precambrian–Cambrian boundary. Geological Magazine, 133(04), 417-428.

Lindsay, J., Brasier, M., Shields, G., Khomentovsky, V., & Bat-Ireedui, Y. (1996). Glacial facies associations in a Neoproterozoic back-arc setting, Zavkhan Basin, western Mongolia. Geological Magazine, 133(04), 391-402.

Macdonald, F. A., Jones, D. S., & Schrag, D. P. (2009). Stratigraphic and tectonic implications of a newly discovered glacial diamictite–cap carbonate couplet in southwestern Mongolia. Geology, 37(2), 123-126.

Maloof, A. C., Porter, S. M., Moore, J. L., Dudás, F. Ö., Bowring, S. A., Higgins, J. A., . . . Eddy, M. P. (2010). The earliest Cambrian record of animals and ocean geochemical change. Geological Society of America Bulletin, 122(11-12), 1731-1774.

Maloof, A. C., Ramezani, J., Bowring, S. A., Fike, D. A., Porter, S. M., & Mazouad, M. (2010). Constraints on early Cambrian carbon cycling from the duration of the Nemakit-Daldynian–Tommotian boundary δ13C shift, Morocco. Geology, 38(7), 623-626.

Maloof, A. C., Schrag, D. P., Crowley, J. L., & Bowring, S. A. (2005). An expanded record of Early Cambrian carbon cycling from the Anti-Atlas Margin, Morocco. Canadian Journal of Earth Sciences, 42(12), 2195-2216.

Markova, N., Korobov, M., and Zhuravleva, Z., 1972, K voprosu o vend-kembriyskikh otlozheniyakh Yugo-Zapadnoy Mongolii (On the problem of the Vendian-Cambrian deposits of southwestern Mongolia): Bulleten'Moskovskogo obshchestva ispytateley prirody, Otdel geologicheskiy, v. 47, no. 1, p. 57-70.

Matthews, S., & Cowie, J. (1979). Early Cambrian transgression. Journal of the Geological Society, 136(2), 133-135.

Mazumdar, A., Banerjee, D., Schidlowski, M., & Balaram, V. (1999). Rare-earth elements and stable isotope geochemistry of early Cambrian chert-phosphorite assemblages from the Lower Tal Formation of the Krol Belt (Lesser Himalaya, India). Chemical Geology, 156(1), 275-297.

McArthur, J., Howarth, R., & Shields, G. (2012). Strontium isotope stratigraphy. The geologic time scale, 1, 127-144.

McKerrow, W. S., Scotese, C. R., & Brasier, M. D. (1992). Early Cambrian continental reconstructions. Journal of the Geological Society, 149(4), 599-606.

Melezhik, V., Pokrovsky, B., Fallick, A., Kuznetsov, A., & Bujakaite, M. (2009). Constraints on 87Sr/86Sr of Late Ediacaran seawater: insight from Siberian high-Sr limestones. Journal of the Geological Society, 166(1), 183-191.

Miller, K. G., Kominz, M. A., Browning, J. V., Wright, J. D., Mountain, G. S., Katz, M. E., . . . Pekar, S. F. (2005). The Phanerozoic record of global sea-level change. Science, 310(5752), 1293-1298.

Moore, C. H. (1989). Carbonate diagenesis and porosity: Elsevier.

Narbonne, G.M., Kaufman, A.J., and Knoll, A.H., 1994, Integrated chemostratigraphy and biostratigraphy of the Windermere Supergroup, northwestern Canada: Implications for Neoproterozoic correlations and the early evolution of animals: Geological Society of America Bulletin, v. 106, no. 10, p. 1281-1292.

Nicholas, C. (1996). The Sr isotopic evolution of the oceans during the'Cambrian Explosion'. Journal of the Geological Society, 153(2), 243-254.

Palmer, M. R., & Edmond, J. M. (1989). The strontium isotope budget of the modern ocean. Earth and Planetary Science Letters, 92(1), 11-26.

Palmer, M. R., & Edmond, J. M. (1992). Controls over the strontium isotope composition of river water. Geochimica et Cosmochimica Acta, 56(5), 2099-2111.

Peters, S. E., & Gaines, R. R. (2012). Formation of the/Great Unconformity/'as a trigger for the Cambrian explosion. Nature, 484(7394), 363-366.

Planavsky, N. J., Rouxel, O. J., Bekker, A., Lalonde, S. V., Konhauser, K. O., Reinhard, C. T., & Lyons, T. W. (2010). The evolution of the marine phosphate reservoir. Nature, 467(7319), 1088-1090.

Porada, H. (1989). Pan-African rifting and orogenesis in southern to equatorial Africa and eastern Brazil. Precambrian Research, 44(2), 103-136.

Porter, S. M. (2007). Seawater chemistry and early carbonate biomineralization. Science, 316(5829), 1302-1302.

Rooney, A. D., Macdonald, F. A., Strauss, J. V., Dudás, F. Ö., Hallmann, C., & Selby, D. (2014). Re-Os geochronology and coupled Os-Sr isotope

constraints on the Sturtian snowball Earth. Proceedings of the National Academy of Sciences, 111(1), 51-56.
Sandberg, P. A. (1983). An oscillating trend in Phanerozoic non-skeletal carbonate mineralogy. Nature(305), 19-22.
Smith, E. F., Macdonald, F. A., Petach, T. N., Bold, U., Schrag, D. P. (in review). Integrated stratigraphic, geochemical, and paleontological late Ediacaran to early Cambrian records from southwestern Mongolia. Geological Society of America Bulletin.
Sawaki, Y., Ohno, T., Fukushi, Y., Komiya, T., Ishikawa, T., Hirata, T., & Maruyama, S. (2008). Sr isotope excursion across the Precambrian–Cambrian boundary in the Three Gorges area, South China. Gondwana Research, 14(1), 134-147.
Shields, G., & Veizer, J. (2002). Precambrian marine carbonate isotope database: Version 1.1. Geochemistry, Geophysics, Geosystems, 3(6), 1 of 12-12 of 12.
Sperling, E. A., Frieder, C. A., Raman, A. V., Girguis, P. R., Levin, L. A., & Knoll, A. H. (2013). Oxygen, ecology, and the Cambrian radiation of animals. Proceedings of the National Academy of Sciences, 110(33), 13446-13451.
Squire, R., Wilson, C., Dugdale, L., Jupp, B., & Kaufman, A. (2006). Cambrian backarc-basin basalt in western Victoria related to evolution of a continent-dipping subduction zone. Australian Journal of Earth Sciences, 53(5), 707-719.
Stanley, S. M. (1976). Fossil data and the Precambrian-Cambrian evolutionary transition. American Journal of Science, 276(1), 56-76.
Steiner, M., Li, G., Qian, Y., Zhu, M., and Erdtmann, B.-D., 2007, Neoproterozoic to early Cambrian small shelly fossil assemblages and a revised biostratigraphic correlation of the Yangtze Platform (China): Palaeogeography, Palaeoclimatology, Palaeoecology, v. 254, no. 1, p. 67-99.
Stoll, H. M., & Schrag, D. P. (1998). Effects of Quaternary sea level cycles on strontium in seawater. Geochimica et Cosmochimica Acta, 62(7), 1107-1118.
Swart, P. K. (2001). The 87Sr/86Sr ratios of carbonates, phosphorites, and fluids collected during the Bahamas drilling project cores Clino and Unda: implications for dating and diagenesis.
Trompette, R. (1996). Temporal relationship between cratonization and glaciation: the Vendian-early Cambrian glaciation in Western Gondwana. Palaeogeography, Palaeoclimatology, Palaeoecology, 123(1), 373-383.

Tucker, M. E. (1992). The Precambrian–Cambrian boundary: seawater chemistry, ocean circulation and nutrient supply in metazoan evolution, extinction and biomineralization. Journal of the Geological Society, 149(4), 655-668.
Veizer, J., Ala, D., Azmy, K., Bruckschen, P., Buhl, D., Bruhn, F., Godderis, Y. (1999). 87Sr/86Sr, δ13C and δ18O evolution of Phanerozoic seawater. Chemical Geology, 161(1), 59-88.
Vinogradov, V., Pichugin, L., Bykhover, V., Golovin, D., Murav'ev, V., & Buyakaite, M. (1996). Isotopic Features and Dating of Epigenetic Alterations of Upper Precambrian Deposits of the Ura Uplift. Lithology and Mineral Resources of Lothologiia I Poleznye Iskopaemye, 31, 60-69.
Vogel, M.B., Ireland, T.R. and Weaver, S.D., 2002. The multistage history of the Queen Maud Batholith, La Gorce Mountains, central Transantarctic Mountains. In: J.A. Gamble, D.N.B. Skinner and S. Henrys (Editors), Antarctica at the close of a millennium. The Royal Society of New Zealand Bulletin 35, Wellington, New Zealand, pp. 153-159.
Voronin, Y. I., Voronova, L., Grigorieva, N., Drosdova, N., Shegallo, E., Zhuravlev, A. Y., Syssoiev, V. (1982). The Precambrian/Cambrian boundary in the Geosynclinal areas (The reference section of Salany-Gol, MPR). Transactions of the Joint Soviet-Mongolian palaeontological expedition, 18, 150.